Bio-inspired synthesis of 45S5 bioactive glass using CT-DNA/GELATIN as template

A Major Project Report submitted in partial fulfillment for the award of the degree of

MASTER OF TECHNOLOGY

In

POLYMER TECHNOLOGY

Submitted by

FARAH ANJUM

(02/PTY/2K10)

Under the esteemed guidance of

Dr. DEENAN SANTHIYA

ASSISTANT PROFESSOR

DEPARTMENT OF APPLIED CHEMISTRY & POLYMER TECHNOLOGY

DELHI TECHNOLOGICAL UNIVERSITY

(*FORMERLY DELHI COLLEGE OF ENGINEERING*)

MAIN BAWANA ROAD, DELHI-110042

DEPARTMENT OF POLYMER TECHNOLOGY AND APPLIED CHEMISTRY

DELHI TECHNOLOGICAL UNIVERSITY, DELHI-42

CERTIFICATE

This is to certify that major report entitled

"Bio-inspired synthesis of 45S5 bioactive glass using CT-DNA/GELATIN as template", is being submitted in partial fulfilment for the award of degree of master of technology in Delhi Technological University. This work was carried out by Farah Anjum (02/PTY/2010) under my guidance and supervision.

Dr. Deenan Santhiya   Prof. G.L.Verma

Assistant Professor   Head of the Department

Delhi Technological University, Delhi   Polymer Technology and Applied Chemistry

Delhi Technological University, Delhi

ACKNOWLEDGEMENT

I would like to express my sincere gratitude and thanks to my project guide Dr. Deenan Santhiya, Assistant Professor, in Department of Polymer Technology And Applied Chemistry, Delhi Technological University for her continuous motivation, encouragement and direction in every stage of this project.

I would also like to thank University of Delhi, Institute of Genomics and Integrative Biology (IGIB) for further extended facilities for this research work and I also like to thank Head of the Department prof. G.L.Verma, my Fellow Mates and Technical staff of the department for their support during the entire duration of project.

Farah Anjum
02/PTY/2010
M.Tech Polymers Science & Technology (4th Semester)
Department of Polymer Technology and Applied Chemistry
Delhi Technology University
Bawana Road, Delhi - 110042

CONTENTS

LIST OF FIGURES

LIST OF TABLES

Abstract

Bioactive glass samples (BIS-BG-D/BIS-BG-G) were synthesized by bioinspired rout using CT-DNA/gelatin as template. Additionally, the bioactive glass named SG-BG-G was also synthesized by sol-gel rout using gelatin as template. The biomaterials were characterized by FTIR, SEM, EDS and XRD. SEM micrographs indicated mesoporous microstructure of BIS-BG-D and XRD analysis confirmed the glass samples which are prepared by bioinspired rout are partially crystalline, whereas the glass sample synthesized by sol-gel rout is amorphous in nature. A few characterization tests like density measurement, swelling tests and in vitro degradation studies were also carried out on all bioactive glass samples prepared. Further glass samples are subjected to in vitro bioactivity test by immersing them in simulated body fluid (SBF) at various time intervals. After interaction with SBF the glass samples were subjected to FTIR, XRD, SEM, EDS analysis, the corresponding SBF solutions were tested for pH and also subjected to elemental analysis by ICP-AES. Interestingly, hydroxyl carbonate apatite (HCA) deposition was observed on the surface of the glass pellets after interaction with SBF and the HCA deposition on the glass surface was further confirmed by FTIR, XRD and EDS analysis. Interestingly, the deposition was found to be higher on BIS-BG-D sample due to its mesoporous microstructure. Hence, further experiments like, pH measurement and elemental analysis of SBF after interaction with the glass and cytotoxicity experiments were carried out only on BIS-BG-D sample. The pH of the SBF solution after interaction with BIS-BG-D was found to decrease from 7 to 8.2 after 7 days and remain constant upto 30 days and the corresponding Ca and P ion analysis showed release of these ions from the glass sample into the SBF solution and indicated the similar trend as observed in the case of pH changes observed. In vitro cytotoxicity experiments carried out on BIS-BG-D glass sample using osteosarcoma cells by following MTT assay method indicated the bio glass sample is of good biocompatibility to serve for third generation scaffold materials.

CHAPTER 1

1. Introduction

With increasing expectancy of human life, an improvement in the quality of biomaterials used for regeneration or repair of hard and soft tissues in the human body become essential. A biomaterial is defined as any systemically, pharmacologically inert substance or combination of substances utilized for implantation within or incorporation with a living system to supplement or replace functions of living tissues or organs [1, 2]. In order to achieve that purpose, a biomaterial must be in contact with living tissues or body fluids resulting in an interface between living and nonliving substances. A broad range of materials including metals, alloys, ceramics, glass ceramic, polymers, glasses and composite materials can act as biomaterials. The first generation of biomaterials, from the early 1970s, can be classified as bioinerts. Designed to minimize any aggressive biological responses by the body, they simply had a mechanical role. During

1980s, a second generation biomaterials defined as bioactive materials were developed. Their key feature is the capability of their surface to interact with physiological fluids to generate a bone-like layer of hydroxyapatite $Ca_{10}(PO_4)_6(OH)$. Human cells grow and proliferate on this layer promoting a tight bond between the implant and the living tissue. Recently, a third generation biomaterials are developed. They can be defined as bioresorbable materials as they react and dissolve in the physiological environment and they eventually replaced by regenerated hard or soft tissue [3]. In present scenario, in addition to accidental bone damages, the number of people also affected by bone diseases such as osteoporosis and is dramatically increasing especially among the aged. As a result, the major clinical application of biomaterials is in the field of treatment of bone defects as bone implants, coating on metallic implants and bone grafting materials [4].

Glasses are widely used from past 3 decades in various technologies due to their many applications as monoliths, fibers or coating. Similarly, glasses are also being used in the field of biomaterials as bioactive glasses. The traditional bio active glasses have silicate network with main structure formed by $(SiO_4)^{4-}$ tetrahedral units linked by bridging Oxygens. Bioactive glasses of silicate composition were first developed by Hench and co-workers in 1969 [5] and had a composition based on SiO_2-P_2O_5-CaO-Na_2O, with silica as the main component, and many of the contemporary analogues, including those generated by sol-gel methods have a SiO_2-CaO based structure. Because of their insolubility, they are used as long-term implants to replace hard or soft tissues. Interestingly, these glasses are known to induce chemical bonding with living tissues by forming a biologically active layer of carbohydroxyapatite (CHA) on their surface [6, 7].

There are well known methods for producing glasses: melting, sintering and sol-gel. The former consists of melting a mixture of inorganic compounds (oxides, carbonates, phosphates etc.) and quenching the melt, while sintering implies the consideration of amorphous powder to form pure glass. On the other hand, the sol-gel method consists of obtaining the sol by consideration of the precursors and gelation of this sol. The sol-gel method presents some advantages with respect to melting. In first

place, glasses are obtained by sol-gel method with a higher degree of purity, with more varied compositions, more easily controlled morphology and better homogeneity [8-11].

In this investigation, we propose to synthesis 45S5 bioactive glass scaffolds by sol-gel as well as bio-inspired rout using natural polymers (gelatin/ Calf thymus-DNA (CT-DNA)) as template. From the literature it is evident that the sol-gel synthetic rout is quite common method to synthesis bio-glasses of various compositions [8-11]. On the other hand, as per our knowledge, bio-inspired synthetic rout is followed first time by us to synthesis bioactive glass.Bio inspired rout was developed by the inspiration on naturally occurring materials such as shell, bones and teeth with outstanding architecture and mechanical properties [12,13]. Literature reveals that bio-inspired synthetic methods are extensively used to develop novel functional nano-sized materials with well-defined 1D and 2D nanostructures using biomacromolecules (e.g. proteins, peptides, amino and nucleic acids), which can serve as templates, scaffolds and stabilizers at room temperature and pressure [14,15]. Similarly, we also expect that bio-inspired method is a simple, cheap and environmentally friendly approach for the synthesis of bioactive glass compared to conventional methods such as melting, sintering and sol-gel methods. These traditional methods for example melting and sintering methods are need of sophisticated instruments, high energy and more raw materials. Whereas, sol-gel methods are in need of toxic chemicals and follow complicated organometallic synthetic strategies. It is also pertinent to mention that similar to sol-gel technique [16], bio-inspired processes also it is possible to fabricate materials in a variety of forms, including ultrafine spherical powders, thin film coating, ceramic fibers, micro porous inorganic membranes, monolithic ceramics and glasses and highly porous aerogel materials but more economically.

The 45S5 bioactive glass contains 45% SiO_2, 24.5% Na_2O, 24.4% CaO and 6% P_2O_5 (in wt. %) and is the best characterized so far especially melt-derived 45S5 bioglass ceramic. This bioglass composition exposes critical concentrations of Ca, Si, Na and P ions which are shown to activate genes in osteoblast (A cell that makes bone. It does so by producing a matrix that then becomes mineralized) cells thus stimulating new bone formation in vivo [17,18].Additionally, 45S5 bioglass has been used in a number of medical devices approved by the US Food and Drug administration (FDA)

[19]. It is interesting to know from literature a few researchers used natural polymers as template to synthesis bioactive glass composites in a variety of forms [20]. In this investigation we used gelatin/CT-DNA as templates to synthesis mesoporous bioactive glass material. Gelatin is the denaturation product of collagen, which is the major structural protein in the connective tissue of animal skin and bone. The protein is rather simple consisting of a highly repetitive sequence of amino acids [(Gly)-X-Y]n, where Gly stands for glycine, X is often proline (Pro) and Y is hydroxyproline (Hyp)[21]. In the past decade, a particularly attractive biological template is the double helix of DNA possessing a linear as well as coiled structure, mechanical rigidity as well as physicochemical stability. It is also pertinent to mention that DNA also been extensively used for controlled arrangement of molecules and nano particles into well-defined nano structured materials [22]. In this investigation, we synthesized mesoporous 45S5 bioactive glass using gelatin/CT-DNA as template by sol-gel/bioinspired rout. The resulting bioglass materials were characterized by analytical and microscopic methods such as XRD, SEM-EDX and FTIR techniques. The bioglass materials were subjected to density, swelling and in vitro degradation tests. Additionally, the bioglass materials were also tested for their corresponding in vitro bioactivity by immersing them in simulated body fluid (SBF). More interestingly, in vivo cytocompatability of the glass materials were also examined using osteoblast cells by MTT assay.

CHAPTER 2

2. Literature Review

2.1 BIOMATERIALS

The biomaterials used in medicine have made a great impact on the treatment of injuries and diseases of human body. Biomaterials use increased rapidly in the late 1800s, particularly after the advent of aseptic surgical technique by Dr. Joseph in the 1860s. Between late 18th to 19th centuries the first metal devices were used to fix bone fractures and the first total hip replacement prosthesis was implanted in1938, and in the 1950s and 1960s, polymers were introduced for cornea replacements and blood vessel replacements. Today biomaterials are used throughout the body as shown in Figure 1.
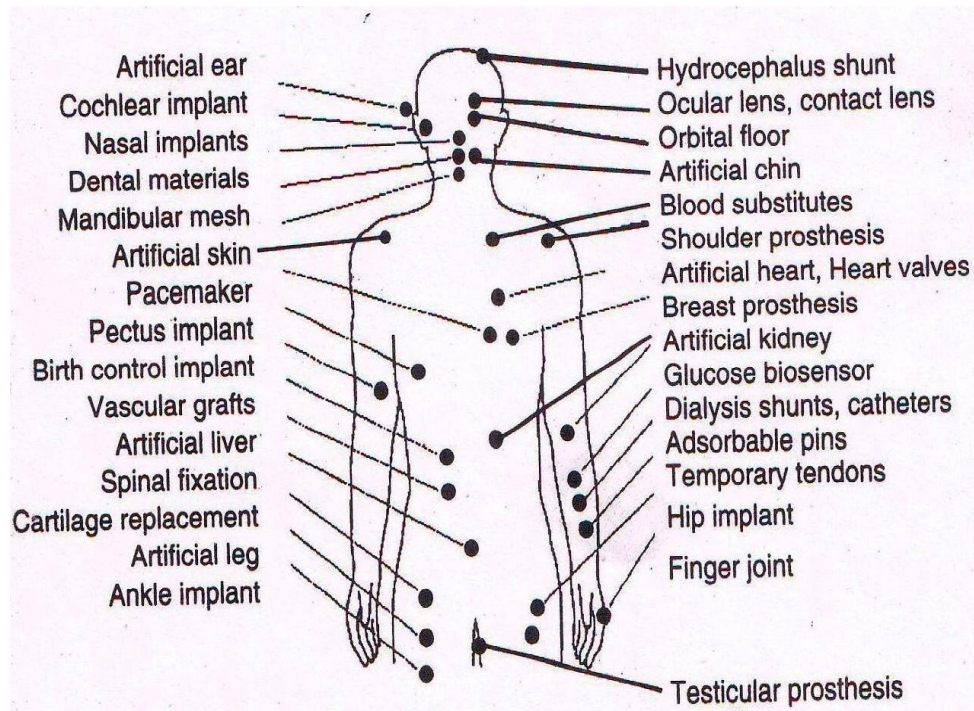
Fig.2.1. A Schematic diagram showing use of biomaterial throughout the body [23].

It is obvious that biomaterials saves millions of lives and quality of life of millions more improved every year due to biomaterials. As we know that there is no single biomaterial available which is suitable for all kind of applications. Therefore this area needs more intensive research and new applications are continually being developed as medicine advances. Understanding of tissues, diseases and trauma improved, the concept of attempting to repair of damaged tissue emerged. Due to the complexity of cell and tissue reactions to biomaterials it has been proven advantageous to observe nature for guidance on biomaterials design, selection, synthesis, and fabrication [2, 23, and 24].

2.1.1. TYPES OF BIOMATERIALS [2, 23, 24, 25-27]

According to Williams, D.F a biomaterial is a nonviable material used in a medical device, intended to interact with biological systems.These materials could be made up of metals, ceramics, polymers and composites (Figure 2.2). The following are a few examples of implants along with their respective biomaterials, by which they are made up of (Figure 2.3).

17
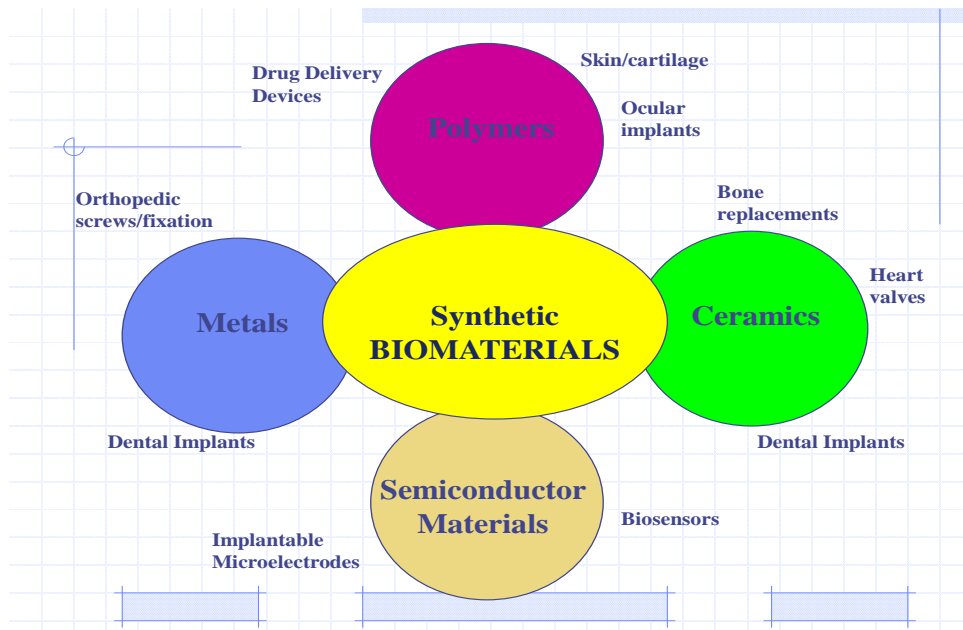
Fig. 2.2. A schematic representation of types of biomaterials along with their applications
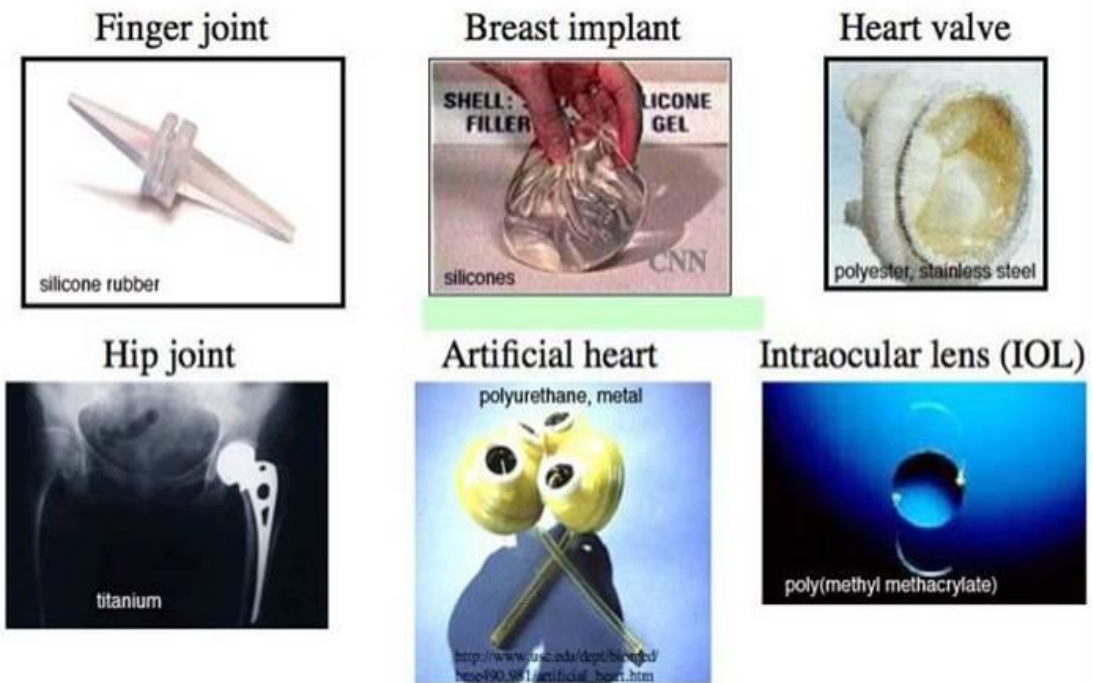
Fig.2.3. Picture of a few implants along with their biomaterials respectively.

Metals

Gold and Iron are examples for the earliest biomaterials used in dentistry and rejoin fractured femur. In general, metals used as biomaterials have high strength and resistance to fracture and are designed to resist corrosion.The advantages of metals over other materials such as ceramics and polymers are strong, tough and ductile. Whereas, disadvantages include susceptibility to corrosion due to the nature of metallic bond [2, 23].For example, many orthopaedic devices are made up of metals, such as hip and knee joint replacement (Figure 2.4). It is pertinent to mention that metallic plates and screw which also hold fractured bones together during healing also are made up of metal.Stainless steel, cobalt alloys and titanium alloys are few examples for metallic biomaterials.

Polymers

Polymers are well suited for biomedical applications because of their diverse properties. Such as flexible or rigid, can be low strength or high strength are resistance to protein attachment or can be modified to encourage protein attachment , can be biodegradable or permanent , and can be fabricated into complex shapes by many methods. Some important disadvantage of polymers are that they tend to have lower strengths than metals or ceramics , deform with time , may deteriorate during sterilization , may degrade in body catastrophically or by release of toxic by – products. Examples of polymers and their corresponding medical applications are listed below [2].

- Nylon-surgical sutures, gastrointestinal segments, tracheal tubes
- Silicon rubber-finger joints, artificial skin, breast implants, intraocular lenses catheters
- Polyester-Resorbable sutures, fracture fixation, cell scaffolds, skin wound coverings, drug delivery devices
- Polyethylene-Hip and knee implants, artificial tendons and ligaments, synthetic vascular grafts, dentures and facial implants.
- Polymethylmethacrylate-Bone cement, intraocular lenses
- Polyvinylchloride-tubing, facial prostheses

Natural materials

The materials, which are synthesized by an organism or plant, are called natural materials. These materials are typically more chemically and structurally complicated than synthetic materials.Protein and polysaccharides are typical examples of natural form of polymers are used in medical devices. There are also ceramic materials. Natural ceramics are typically calcium based such as calcium phosphate bone crystals or calcium carbonate coral or sea shells. Natural ceramics are typically much tougher (resistant to fracture) than the synthetic ceramics due to their highly organized microstructure which prevent crack propagation. In natural ceramics, small ceramics crystals are precisely arranged and aligned and are separated by thin sheets of organic matrix material (Figure 2.5). Natural materials exhibit a lower in incidence of toxicity inflammation as compare to synthetic materials. However, it is often expensive to produce or isolate natural materials.Some of natural materials and the corresponding biomedical applications are listed below:

- Collagen and gelatin-cosmetic surgery, wound dressing, tissue engineering, cell scaffold

- Cellulose-Drug delivery

- Chitin-Wound dressing, cell scaffold, drug delivery

- Ceramics or demineralized ceramics-Bone graft substitute

- Alginate-Drug delivery, cell encapsulation

- Hyaluronic acid-Postoperative adhesion prevention, ophthalmic and orthopedic lubricant, drug delivery, cell scaffold

Fig.2.4. Hip and knee joint metallic implants [2, 23].
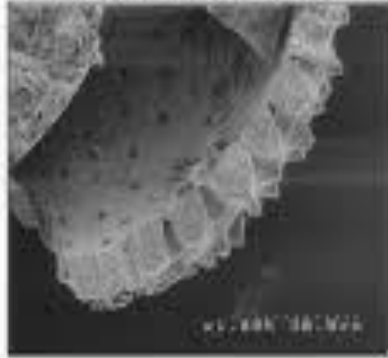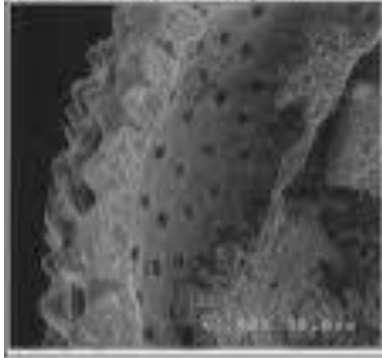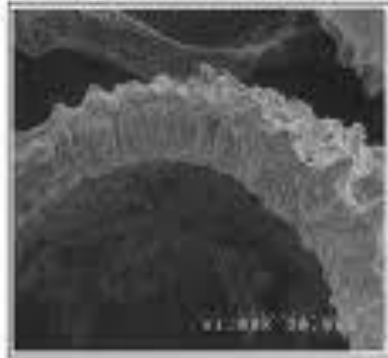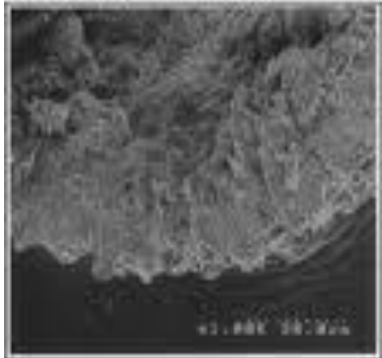
Fig.2.5. A picture of sea shell and its SEM micrograph [28].

Ceramics [25]

Ceramic biomaterials are referred to as bioceramics, since they are used for repair and replacement of diseased and damaged parts of the musculoskeletal system. Various types of ceramics, which are used as biomaterials are briefed in Table 2.1.

Table 2.1. Ceramics used in biomedical applications [2]

Ceramics used in Biomedical Applications		
Ceramic	Chemical Formula	Comment
Alumina	Al_2O_3	Bioinert
Zirconia	ZrO_2	
Pyrolytic carbon		
Bioglass	$Na_2OCaOP_2O_3-SiO$	Bioactive
Hydroxyapatite (sintered at high temperature)	$Ca_{10}(PO_4)_6(OH)_2$	
Hydroxyapatite (sintered at low temperature)	$Ca_{10}(PO_4)_6(OH)_2$	Biodegradable
Tricalcium phosphate	$Ca_3(PO_4)_2$	

Since, this M.Tech dissertation is on the synthesis of bioglass material for bone implants, the following discussions are focused on bone and its related information.

2.2 BONE STRUCTURE [23, 24, 29, 30]

Bone comprises a network of collagen fibers that are impregnated with crystals of hydroxyapatite i.e. $Ca_5(PO_4)_3(OH)$, and some Calcium Carbonate. Collagen is a flexible, tough protein that dictates the shape of the bone, to which the hydroxyapatite phase is bonded via polar functional groups on the protein molecules and provides additional strength. The channels carry blood vessels, nerves and lymphatic are enclosed within this solid collagen-mineral matrix. The Structure of bone is depicted in Figure 2.6. Long bones, such as the femur*,* comprise an exterior, relatively rigid, dense 'cortical' bone with a compressive strength of 100-230 MPa and a young's modulus of 7-30 GPa. The interior of this bone consists of a spongy, honeycomb-like structure composed of the

collagen-mineral matrix filled with soft marrow, fat and bone cells. This porous 'trabecular' bone is comparatively weak and more flexible than cortical bone, having a compressive strength and young's modulus of 2-12 MPa and 0.05 - 0.5 GPa, respectively. The specific arrangement of cortical and trabecular bone, and the difference between their mechanical properties provides a smooth stress gradient from tendon to bone and mediates the transfer of forces along the bone.

The structure and function of bone is maintained by a balance between the activities of bone-forming cells - osteoblasts - and the bone resorbing cells - osteoclasts. A reduction in the normal stress patterns exerted on bone causes demineralization (also known as bone atrophy) during which osteoblast activity diminishes, causing a net resorption of hydroxyapatite and Calcium Carbonate by the body. Bedridden patients, sedentary elderly people and astronauts are particularly prone to reduced mechanical stress on their bones and the consequential loss of bone density. The effects are particularly severe in trabecular bone and greatly reduce its mechanical strength and resistance to fracture. The trabecular bone is also vulnerable to demineralization with ageing. In a study of the human femur, tensile strength was found to decrease from around 120 MPa to 65 MPa from the ages of 20 to 95 years.
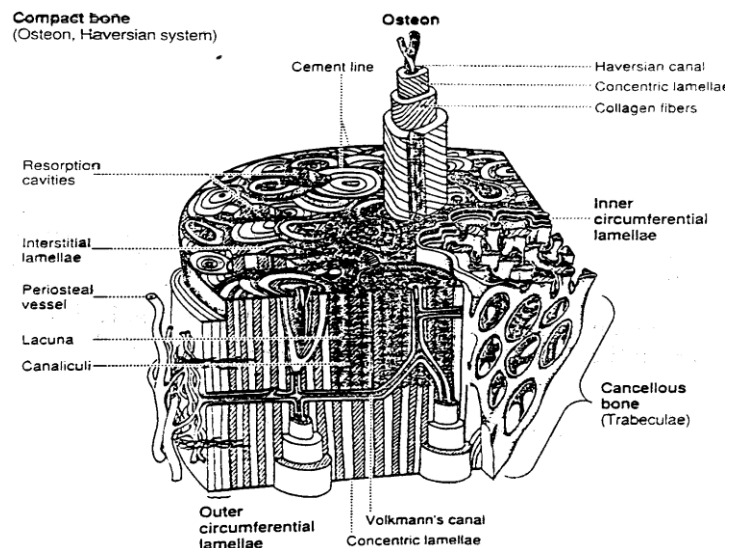
Fig.2.6. Structure of Bone [31].

2.3 TISSUE- BIOMATERIAL INTERACTIONS [23,24]

When biomaterials are implanted in body many of the components present in body fluid for example blood interact with implant and give positive or negative response to body.

2.3.1 INTERACTIONS WITH BLOOD AND PROTEINS [23,24]

The implantations of a biomaterial often create a wound and followed by bleeding. Blood thus typically makes first contact with the implanted biomaterial. Blood is a mixture of water, various kinds of cells and cell fragments (platelets), salts, and proteins (plasma). Change in levels of proteins or the structure of proteins in blood lead to altered function of tissues and are responsible for a variety of diseases. Hence, blood screening for certain proteins is essential to indicate a diseased state or cancer.

Platelets from the blood will adhere to the biomaterials, which leads to fibrin clot formation. The time, at which the protein attachment begins, a cascading chain of cellular reactions is also governed by the protein. Hence, Blood contact provides the cells and cytokines that participate in the biological interaction with the biomaterial. Therefore, every biomaterial that contacts blood will elicits biological responses from the body.

2.3.2. THE WOUND HEALING RESPONSE AFTER BIOMATERIAL IMPLANTS [23,24,32,33]

The implantation of a biomaterial creates a disruption of anatomic continuity of tissue and as such creates a wound healing response that is immediately triggered by the biomaterial implantation. From the prospective of tissue–biomaterial interaction, there are four overlapping phase.

Haemostasis: Platelet cells control bleeding through coagulation. The clot that is formed acts as provisional matrix for the initiation of repair tissue and fills the gaps around the implanted biomaterial.

Inflammation: The clot formation induces the cell signaling molecules (cytokines) that induce the recruitment of inflammatory cells from the nearby blood stream. These cells digest tissue debris and biomaterial by a process called phagocytosis. The wound site inflammatory cells initiate mitosis (cell replication) of sedentary connective tissue cells at the wound margin.

Proliferation: These inflammatory cells begin the damage tissue formation. If biomaterial is non-degradable, biomaterial located in the center of the wound typically becomes encapsulated with tight fibrous tissue. Whereas, in the case of degradable implant, degradation takes place simultaneously during the tissue formation.

Remodeling: The rapidly formed neotissue (newly formed tissue) will be remodeled by cells into functional tissue more similar to the original tissue.

2.4. BIOMATERIAL DEGRADATION AND RESORPTION [3,34]

It is well known that biomaterials may be permanent or degradable, which may be chemically driven or accomplished by cells. Bioresorbable implants are designed to degrade gradually over time in the biological environment and be replaced with natural tissues. The goal is to meet the requirements of strength and cell support while the regeneration of tissue is occurring. Small changes in biomaterial chemistry and structure may greatly alter the resorbtion rate, allowing for materials to be tailored for various applications or leading to unexpected product failure. Collagen and the Lactic acid and /or Glycolic acid polymers (PLLA and PGA or copolymer PLGA) are the most commonly used polymeric biomaterials for resorbable applications. As a result of resorbtion, the Lactic acid and Glycolic acid fragments are eventually metabolized into carbon dioxide and water. Whereas, tricalcium phosphate a biodegradable ceramics, degrade through a surface dissolution process into calcium and phosphate salts, which are also present naturally in the body.

2.5. Tissue Repair [3,35]

The promotion of new tissue deposition importantly needs the interaction of cells and tissues with the biomaterial surface. There are many ways to control cell-surface

interactions namely by immobilizing essential proteins for cell growth on the biomaterial surface (biomimetic approach), modification of surface topography of biomaterial (providing rough, porous coating or grooved surfaces to achieve bony in growth) and using scaffold biomaterial (porous biomaterial). Since the present investigation focuses on the synthesis of porous bioactive glass, a detail discussion on scaffolds is provided in the present section.

2.6. SCAFFOLDS [36,37]

Tissue repair of large defects is best accomplished by filling the defect space with a scaffold material that can simulate the micro environment provided by the embryonic extra cellular matrix. The following are the functions that a scaffold must serve: it must provide sites for growth factor attachment, cell migrations and attachment, a new tissue deposition. Either natural tissue or synthetic tissue analogies are needed to reconstitute a functioning vital tissue. The goal of a scaffold is to recreate important aspects of the cell micro environment that will allow cell proliferation, differentiation and synthesis of extra cellular matrix. One of the most critical elements scaffold biomaterial that it mimic the extra cellular matrix scaffold that normally serve to maintain space , support cell , and organise cell into tissues.

Pore size is a very important parameter of biomaterial scaffold used for tissue regeneration. Through trial and error, optimal ranges of pore sizes have been determined for different tissues and for different biomaterials. There are now some rules of thumb, such as the pores must be at least 5-10 µm for a cell to fit through. Successful bones scaffolds typically have pores that transverse the full thickness of scaffold and are 100 to 250µm in size.

The pore size determines many aspects of scaffold, such as mechanical strength and permeability to gases, fluids and nutrients, in addition to cell ingrowth. Inter connected porosity is essential for tissue engineering applications requiring nutrient diffusion and tissue ingrowth. A highly porous material degrades more quickly than a solid block of material [38].

Tissue engineering is a branch of science, which seeks to promote the regeneration ability of host tissue through a designed scaffold that is populated with cells and signaling molecules. The specific criteria for an ideal scaffold, which is used in bone tissue engineering, are given below:

(i) Ability to act as template for in-vitro and eventually in -vivo bone growth in three dimensions; to fulfill the criteria the scaffold must have an open porous structure to allow cell penetration, tissue ingrowth and eventually vascularization on implantation.

(ii) Resorbability should be at the same rate as the bone is repaired, with degradation products that are non-toxic and that can be easily be excreted by the body. Such resorbable porous polymeric scaffolds have been currently developed. Bone cells may initially attach to polymer scaffolds in-vitro, especially if attachment specific proteins are incorporated on their surface. However, polymers do not bond to bone and do not stimulate cells at the genetic level. Commonly used polymer is Polyglycolicacid, which has the young modulus much lower than bone and degrade rapidly, reducing the strength of the scaffolds before tissue can regenerate.

(iii) Highly biocompatible (not toxic) and promote cell adhesion and activity, stimulating osteogenesis at the genetic level.

(iv) Ability to bond to the host bone without the formation of scar tissue, creating a stable interface.

(v) Appropriate mechanical properties matching that of the host bone after in-vitro tissue culture.

(vi) Irregular shape fabrication ability to match that of the bone defect.

(vii) Commercially producible and sterilizable to the required international standards for clinical use.

It is evident from the literature that bioactive glasses meet the above essential criteria required for a scaffold and serve as a promising scaffold material for bone tissue engineering. It is pertinent to recall that the concept of bioactive material is midway

between those of inert material (remain in the living system without any noticeable change) and resorbable material, which undergo gradual dissolution by the bio-system of the organism and replaced without toxicity and rejection (Table 2.1).

2.7. BIOACTIVITY [24, 39,40]

Bioactivity is an interfacial response of the tissue towards biomaterial, which results at the end in a tissue bonding. On bone, the bioactivity of biomaterial can be subdivided into two parts. First one is osteoinduction that is a tissue activity to the repair or growth of the damaged part of the body due to the ions freed in the biological environment. Secondly, osteoconduction, the process by which bone is directed so as to conform to the surface of the materials. Bioactive materials can be subjected to bioresorption. The process of removal of material for biodegradation exercised by the biological environment is called bioresorption. On the other hand the material can exhibit bio stability (the capacity of a material to resist changes in a biological environment). For example, hydroxyapatite, being similar to the stable product present in the bone, is thermodynamically stable in that environment and so bio-stable in bone while tricalcium phosphate is slowly bioresorbed (except for extensive volumes in which the surface become enveloped by a layer of hydroxyapatite which stops any further dissolution of the interior parts). Bioresorbable ceramics usually have high osteoinduction capability, while hydroxyapatite confers to the surface good bio-attachment and bio-adhesion (the state resulting between tissue and material from mechanical or chemical attachment, respectively). The use of hydroxyapatite is recommended not only for its total bio-tolerability, but also for its ability to influence the growth of neoformation bone and to become involved in it (bioactivity).

2.8. HISTORY OF BIOACTIVE GLASS [41]

Larry L. Hench and colleagues at the University of Florida first time developed these materials in the late 1960s. Initially, Hench work was focused on glass materials and it interaction with nuclear radiations. U.S. army colonel challenged to develop bioactive to regenerate bone, as many Vietnam War veterans suffered badly from bone damage such that mostly injured veteran lost their limbs.

2.9. NEED FOR BIOACTIVE GLASS [2,23,24]

Degenerative bone disease is a growing problem throughout the world. Approximately 90 per cent of the population over the age of 40 suffers to some extent with this condition. While normal repair processes fail with age, injury, infection or excessive loading may also be contributory factors. Moreover, life expectancy in prosperous parts of the world currently stands at 80+ years, which means that many people will exceed the natural lifespan of their own connective tissues, particularly bone and cartilage. Current statistics reveal that 33 per cent of women and 17 per cent of men, between the ages of 80 to 90, get hip fractures.

A general problem with artificial replacement joints - usually a polished metal ball mounted on a metal femoral stem and a polymer or alumina cup - is that of stress transfer from synthetic materials, whose mechanical moduli (elasticity) are very different from that of the host bone. Changes in mechanical loading following hip replacement cause demineralization of bone from the inner wall of the femur, which can lead to loosening of the femoral stem. Additionally, wear debris from the articulating prosthetic joint is also a common problem that provokes the body's immune response and tends to require revision surgery. While bone transplantation is an alternative, the lack of donors and tissue compatibility limit the usefulness of this approach. Current research is focusing on the design of bioactive glass and ceramic scaffolds that could be used to enhance the body's own repair mechanisms, and thus regenerate compromised bone tissue in situ.

2.10. COMPOSITION OF BIOACTIVE GLASS [41-43]

The first bioactive glass was developed by Hench et al. and was named bioglass 45S5. The 45S5 glass exhibits at high bioactivity and can join readily even to soft tissues. This is the most widely studied bioactive glass. The 45S5 name signifies glass with 45% of SiO_2 and 5:1 ratio of CaO to P_2O_5. This key composition features of bioglass that is less than 60 mole percent SiO_2, high Na_2O and CaO contents, high CaO / P_2O_5 ratio, makes bioglass highly reactive to aqueous medium and bioactive. The composition of Bioglass 45S5 in three different microstructural forms such as amorphous, partially

crystalline and fully crystalline was studied both in vitro and in vivo. All implants examined bonded to a rat femur model within 6 weeks. From 45S5 bioglass Hench et al. also developed and characterized a large series of glasses based on the SiO_2-CaO-Na_2O-P_2O_5 and are listed in Table 2.2. All were characterized in terms of a bioactivity index, which was defined as the time needed for 50% of an implant surface to attach to bone ($t_{0.5}$) i.e. $I_B = [100/t_{0.5}]$ (days^{-1}).

Table 2.2. Composition in wt. % of some glasses [41]

Bioglass	SiO2	CaO	Na_2O	P_2O_5	B_2O_3	CaF_2	K_2O
45S5	45	24.5	24.5	6.0			
45S5F	43	12.0	23.0	6.0		16	
45B15S5	30	24.5	24.5	6.0	15		
45B5S5	40	24.5	24.5	6.0	05		
KCP1	45	24.5		6.0			24.5
45S5-N	50	24.5	19.5	6.0			
45S5-C	50	19.5	24.5	6.0			

2.11. STRUCTURE OF BIOACTIVE GLASS [41-42]

Bioactive glasses have random network of silica tetrahedral comprising Si-O-Si bond. This network can be modified by introducing the Calcium, Sodium and Phosphorus, which are bonded to network via non-bridging oxygen bonds. The mechanism of bone bonding to bioactive glasses is due to the formation of the carbonated substituted hydroxyl carbonate apatite layer (HCA) on the surface of material when it is immersed in the body fluid. This layer is similar to apatite layer to the bone.

2.12. REACTIVITY OF BIOACTIVE GLASS IN PHYSIOLOGICAL MEDIA [42]

To bond to bone, a hydroxyapatite layer must form on the surface of the implanted material. This is similar in composition and structure to the apatite phase present in bone and having formed, it provides a focus for the deposition of collagen fibrils and for the attachment of stem cells. These cells then differentiate into osteoblasts and initiate the natural bone-building process.

Under normal physiological conditions, our body fluid is highly saturated with the components of hydroxyapatite so, once apatite nuclei are formed, they will grow spontaneously. Additionally, the dissolution of ions, such as Ca^{2+} and PO_4^{3-}, from the glass will increase the degree of saturation of body fluid and enhance the kinetics of hydroxyapatite precipitation.

The mechanism of hydroxyapatite formation on the surface of the first generation of melt-derived bioactive glasses is described in five steps as follows [43] with suitable diagrams.

1. Rapid diffusion-controlled ion exchange of network modifying Ca^{2+} and Na^+ ions from the glass with H_3O^+ ions from the body fluid. This step increases the pH at the implant-bone interface.

$$Si–O–Na^+ + H^+ \rightarrow Si–OH + Na^+ \text{ (aq)}$$
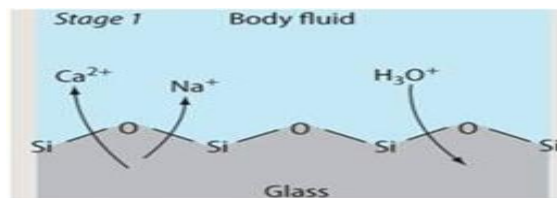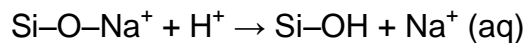
2. Development of silanol groups (Si-OH) at the surface via the partial dissolution of silica at the interface.

$$-OH$$
$$Si–O–Si + H_2O \rightarrow Si–OH + HO–Si$$
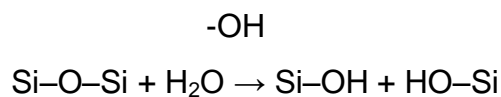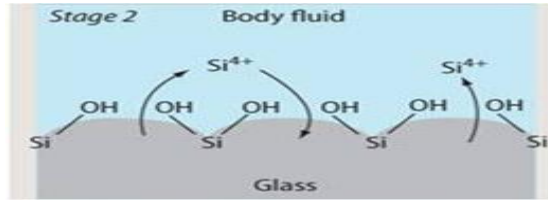
3. The condensation and repolymerisation of the silica-rich surface layer to form an amorphous calcium silicate layer.

$$-OH$$
$$Si–O–H + Si–O–H \rightarrow Si–O–Si + H_2O$$
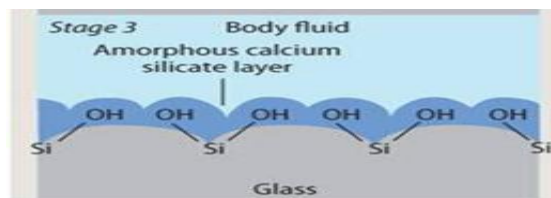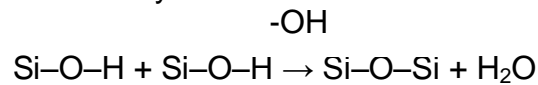
4. Incorporation of HPO_4^{2-} and Ca^{2+} ions from the body fluid into the calcium silicate layer to form an amorphous calcium phosphate layer.
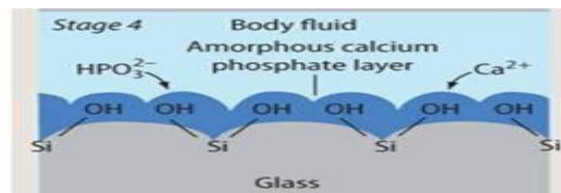
5. Crystallization of the amorphous calcium phosphate layer into biologically equivalent hydroxyapatite.
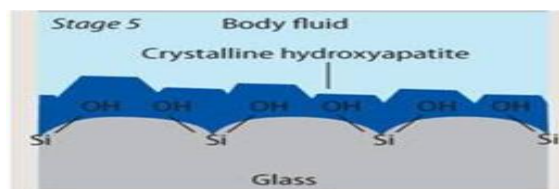
Fig.2.7. Schematic representation of various steps involved in the reactivity of bioactive glass in physiological media [42].

2.13. MECHANISM OF BIOACTIVE GLASSBONDING TO LIVING TISSUES [7,44,45]

The surface of an implanted bioactive glass is known to undergo the five steps described above irrespective of the presence of tissue. However, bonding between a tissue and bioactive glass implant needs additional interfacial reactions, which occur in the following sequence:

a) Adsorption of biological components on the CHA layer

b) Action of macrophages

c) Bonding of stem cells

d) Differentiation of stem cells

e) Generation of matrix and

f) Mineralization of the matrix

The biological processes involved in the above mentioned steps are not well understood till today. Even though based on the analysis of the interface between Bioglass and tissue a few researchers climb that initially collagen fibres provide scaffolding with the sites required for the micro-nucleation of apatite crystals, taking place an inter digitation of the collagen with surface of the material. Apatite crystals grow epitaxial across the bone-implant interface; this means in bone biology terms, that CHA crystals grow oriented along the collage fibres.

2.14. PREPARATION OF BIOACTIVE GLASS

Literature reveals a numerous methods have been followed to prepare bioactive glass. Here, we discuss most used methods and their disadvantages

2.14.1. Melt – Derived Method [46]

The original Bioglass was produced by melt processing, which involves melting high-purity oxides (SiO_2, Na_2CO_3, $CaCO_3$, and P_2O_5) in platinum crucibles in a furnace at 1370°C [38]. Bioglass can be poured into preheated (350°C) moulds (e.g. Graphite) to

produce rods or as-cast components. Bioglass particulate is made by pouring the melt into water to quench, creating a frit. The frit is then dried and ground to the desired particle size range. Compositions that exhibit slower rates of bonding lie between 52 and 60 wt% SiO_2 in the glass. Compositions with greater than 60 wt% SiO_2 are bioinert. Adding multivalent cations, such as Al^{3+}, Ti^{4+} and Ta^{5+}, to the glass shrinks the bone-bonding field.

Disadvantages of Melt – Derived Method

Pores in melt –derived bioactive glasses are few in number and are in the form of oriented channels of irregular diameter through the glass so interconnectivity is poor; it means glasses are not homogenized [46].

2.14.2. SOL- GEL METHOD [1-3]

The sol–gel process involves the hydrolysis of alkoxide precursors to create a sol or colloidal liquid. In the case of silicate based bioactive glasses, the silicate precursor is an alkoxide such as tetraethyl orthosilicate (TEOS). If components other than silica are required in the glass composition, they are added to the sol either as other alkoxides or as salts. Phosphate and calcium are incorporated by adding triethyl phosphate (TEP) and calcium nitrate tetrahydrate, respectively. The sol can be considered as a solution of silica species that can undergo polycondensation to form the silica network of Si–O–Si bonds. A gel forms within three days at ambient temperature. Water and ethanol, which are by-products of the condensation reaction, must be evaporated by using carefully controlled low heating rates. The final step is to heat the dried gel to at least 600°C in order to remove organic by-products.

Sol–gel glasses have a specific surface area, typically ~200 m^2g^{-1}, about two orders of magnitude greater than that of melt-derived glasses. This is because gel glasses contain a nanoporous network that is inherent to the sol–gel process, whereas melt-derived glasses are fully dense. The nanopores in sol–gel glasses are usually in the range of 1–30 nm in diameter. The nanopore size can be tailored during processing by controlling the pH of the catalyst, the nominal composition and the final temperature [24].

Advantages of sol – gel method over melt- derived method

Sol-gel is extremely versatile process, using the sol-gel process, ceramics and glass materials can be fabricated in verities of form including ultrafine spherical powders, thin film coatings, ceramics fibre, micro porous inorganic membrane, monolithic ceramics and glasses and highly porous aerogel material [47]. Advantages of sol–gel bioactive glasses over melt-derived glasses of similar composition are that they are generally more bioactive and can remain bioactive with silica contents of up to 80 mol%. The enhanced bioactivity is due to the nanoporosity and enhanced surface area,which cause increased rates of dissolution. Sol–gel glasses can, therefore, be considered truly bioresorbable. Gel glasses can also be bioactive while containing fewer components, e.g. Glasses composed of 70 mol% SiO_2 and 30 mol% CaO (70S30C) form an HCA layer as rapidly as the 58S glass.

The reason that 70S30C glass can nucleate an HCA layer even though it does not contain phosphate is that Si–OH groups are thought to play a role in HCA layer nucleation. These groups form during the bioactivity mechanism (glass corrosion), but in sol–gel glasses there are several Si–OH groups present in the unreacted glass that can quickly act as nucleation sites. HCA layers can be nucleated on various materials that have a high concentration of surface OH groups when the materials are placed in supersaturated solutions. Sol–gel glasses inherently contain a substantial number of OH groups in the glass network. The glass network is therefore not completely cross linked. Hence, several sol–gel silica-based glasses have nanoporosity, often micro porosity, which causes the high surface area. The higher surface area causes more rapid dissolution than with dense bioglass, even though sol–gel glasses have a higher silica content and greater network connectivity.

A further advantage of sol–gel glasses is that their surfaces can be modified by a variety of surface-chemistry methods, e.g. with amine groups, which can make the surface hydrophobic and attractive to specific proteins. Specially designed proteins can also be attached the material surface prior to implantation to obtain novel bioactivity by delivering the proteins to the desired wound site [1-3].

Disadvantage of Sol-Gel Techniques

Na_2O in a sol-gel bioactive glass provide a technical challenge due to the high hydrolytic reactivity of sodium alkoxide in water. But inclusion of Na_2O provide in improvement in mechanical properties losing the satisfactory biodegradability. If the crystallization is more than 60 percent than it reduces the surface rate of reaction [43], initially Na_2O is use to reduce the melting point of silica-based glass. Sol-gel fabrication of glasses employs organic solvents, which are expensive and non-biofriendly in nature [24].

Although the sol-gel foaming process yield ideal pore network for bioactive glass scaffold, the logical step is to introduce a polymer phase into this process. There are involvements of complex chemistry challenges associated with this procedure these include:

- Choice of polymer

- Calcium precursor

- Removal of toxic by-product

Many bioresorbable polymers cannot be introduce in the sol because of stability issue. To remove the nitrate required temperature 600°C.at this temp polymer phase can be damage.

2.15. COMPLEX MATERIALS [12-14,28]

Complex materials are widespread in nature and have been around for a very long time. But what are complex materials? Since artificial complex materials are still to be developed, looking into natural materials like bone, teeth, diatoms and seashells is the best way to find out what a complex material really is. Alike these biological structures, complex materials are those as shown in Figure 2.8.

a. That exhibit a hierarchically organized structure made up of self-assembled building units ranging from nanometres to millimetres in size,

b.   That intimately combine organic molecules, inorganic matter and living cells in one single system,

c.   That are capable of interacting, self-healing, evolving and adapting in response to external stimuli, and

d.   That has a structure intricately designed and optimized to fulfil multiple specific functions.

Combining these exquisite features into one single material has been so far only possible through biomineralization processes mediated by living cells. While man-devised processing tools are still primitive compared to nature's biomineralization processes, we believe that novel processing strategies can be developed to enable the fabrication of artificial complex materials that capture some of the unique features of rigid biological structures. The ability to create such complex structures in a reproducible and controlled manner using a vast repertoire of chemical compositions should lead to a new generation of smart, functional materials and devices.
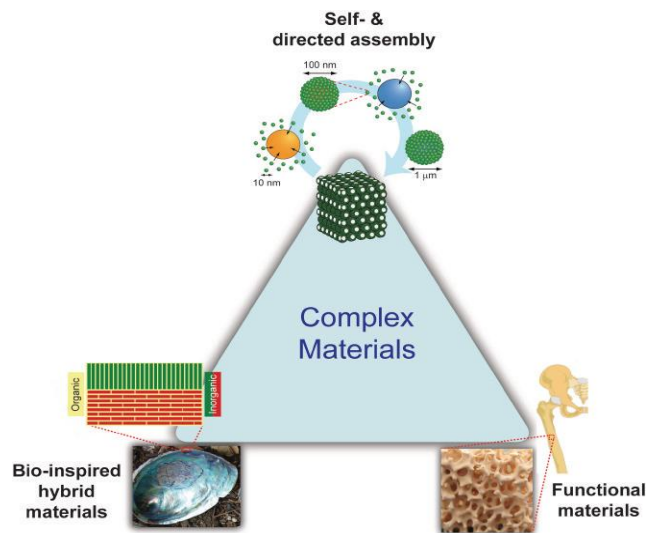
Fig.2.8. Representing the complex materials triangle[28]

2.16. BIO-INSPIRED METHOD [28]

There is considerable interest in simple, cheap and environment friendly approach to produce the bioactive glass as scaffold that would be capable of forming glass and improved the properties. In this approach, emphasize on the low generation of waste and low consumption of material and energy. In this way bio inspired way developed. It represent the typical low temperature, normal pressure atmospheric process, thus the temperature sensitive substrates be used [28].The comparison between shapes and size of the crystals can be controlled by bio-inspired way and other synthetic methods are shown in Figure 2.9.

'Non-biological' crystals   Biominerals
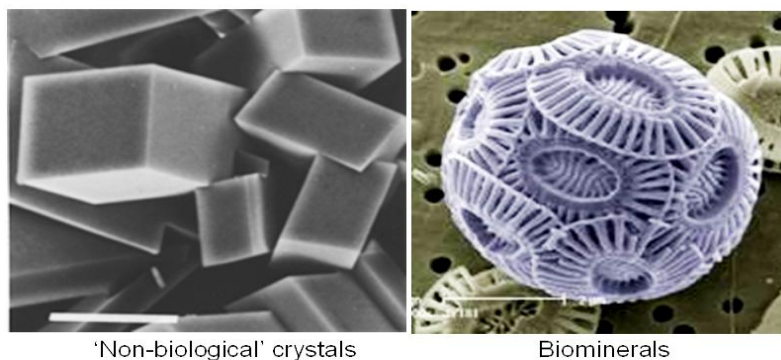
Fig. 2.9. Comparison between shapes of non-biological crystals and bio minerals [28]

Naturally occurring material such as shells, bone and teeth with outstanding properties are some of the examples of biological control mineralization. These are composite materials and consist of combination of inorganic and organic types. Here, small amount of proteins control crystal growth and shape of inorganic part of the composites. Thus biological synthesised materials possess a very high quality and special functionality developed through natural selection. Therefore many researchers are intensively investigating the interactions between inorganic and organic substance and influence one type of the substance on others as shown in following Figures 2.9 and 2.10.

Fig.2.10 (a). Picture of a shell [28].
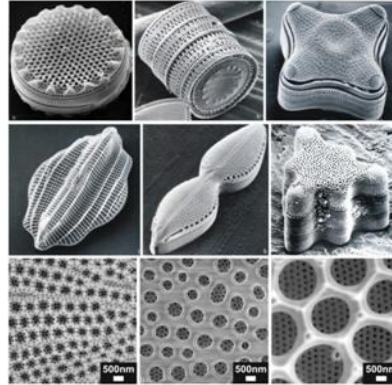
Fig.2.10 (b). Microstructures of hard tissue but variations occur within the structure due to bio-mineralization [28].

The organic template or additives used are synthetic polymers, amino acids and small peptides. These materials have simple chemical structure stable at broad range of temperature, solvent and pH. Although proteins are the organic component found in naturally occurring composites, they are rarely used as additives in crystal growth of inorganic materials. This is because of their complex chemical composition and three dimensional structures, which is extremely sensitive to variation in pH and temperature.

Nevertheless, the investigation of the role of proteins in synthesis of composites can lead to important information about bio mineralization. They are unique macro molecules with different no nature of binding sites which can adsorb metal ions stereo selective by multi point attachment. Hence they are more effective than molecules with lower molecular weight. In the same way we can also use DNA as template in synthesis of inorganic crystals.

2.17. RESEARCH AND DEVELOPMENT ON 45S5

Since the focus of the present investigation is on the bioactive glass of formulation 45S5, we would like to highlight research and developments carried out on the same. 45S5 glass has attracted a serious attention of many researchers due to its excellent bone bonding ability [5,17,26]. Interestingly, 45S5 particulates show remarkable

performance in middle-ear prostheses, jaw, face and nose reconstruction, dental and non-or low load bearing implants most importantly in the repair of periodontal defects [46-48]. 45S5 bioglass granules have also been used to fill and repair defects in osteoplastic frontal sinus surgery [49, 50]. It is pertinent to mention that growth of bone in sinus surgery as well as periodontal defects is accompanied by antimicrobial effects due to the alkaline environment created by the initial ion release from the glass surface [49,50].   In addition to this, the powder biogalss material is shown to serve as a substrate on which osteogenic stem cells can attach and differentiate. Such method of growing 3-D tissues at outside the body is one of the exciting routes to exploit the 3rd generation biomaterials and known as in vitro tissue engineering [51,52]. After implantation the tissue-engineered matrix is expected to degrade slowly, while being repaired by connective tissues which integrate that new tissue into the damaged site [3,53]. Hence the tissue-engineered matrix should preferably make up of non-toxic products indicating the importance of manufacturing process.

So far 45S5 glass is manufactured at various forms by melting and quenching as well as sol-gel techniques by many researchers [48,54-56]. It is pertinent to mention that the characterization and evaluation of melt-derived 45S5 bioglass ceramics are well documented in literature [51,57-60].Currently, researches show much interest on sol-gel process, for example D. Carta et al.[61] fabricated SiO_2-CaO-P_2O_5-Na_2O glasses by preparing the sol of alkoxide precursors of SiO_2-CaO-P_2O_5-Na_2O in ethylene glycol solution under nitrogen atmosphere. Recently, Q. Z. Chen synthesized fine powders of 45S5 glass ceramic using sol-gel technique in aqueous solution under ambient conditions [62]. Additionally, Importance of crystallinity of 45S5 glass in bringing out its mechanical strength is well brought out by a few researches [51,57,58,63,64]. Transformation of bioactive glass 45S5 to a glass ceramic with crystalline phase $Na_2Ca_2SiO_2$ is achieved by heating the material 700 ^{o}C for more than 0.5 h [51,65]. In contrast to mechanical stability due to crystallinity of 45S5, it is shown that formation of hydroxylcarbonate apatite (HCA) takes nearly three times more compare to amorphous counterparts. Interestingly, such time limitation in the formation of HCA is overcome by changing the texture of the crystalline 45S5 glass to increase its surface area [56,66].

It is interesting to highlight that increasing the specific surface area and pore volume of bioactive glasses of various composition are shown to alter remarkably the deposition of HCA and therefore enhances the bioactivity of the materials. For example, ordered mesopores bioactive glasses are demonstrated to be excellent candidates as bone reconstruction materials [67-72]. More importantly, these materials can be loaded with a mass of osteogenic agents or drugs, which could contribute significantly to promote the new in vivo bone growth. In addition to this, mesoporousbioglass materials are shown to be used for bone tissue regeneration [73-75]. Based on the literature it is evident that mesoporousbioglass materials are mostly synthesised by templating polymers and are shown to be superior to normal sol-gel derived biogalss materials [76-82]. For example,3D porous scaffolds based on the original melt derived BG45 is fabricated using special methods, which additionally yield enhanced mechanical properties due to partial crystallisation of the glass [51].These scaffolds are synthesised using replication technique, to achieve mechanically stable 3D scaffolds through a tailored sintering schedule, and to assess the bioactivity of the scaffolds [51].

A few researches also examined the changes in pH and ion concentration of the surrounding fluid such as deionized water, phosphate-buffered saline (PBS), simulated body fluid (SBF) and DMEM tissue culture medium [55,58,59,83-85].Kokubo and Takadama [86] showed the importance of a particular concentration of ions in SBF is essential in predicting in vivo bone formation. Xynos I. D. et. al. and O. Tsigkau et al. demonstrated explicitly that the ions released by partial dissolution of 45S5 activate genes that promote differentiation and proliferation of osteogenic cells [87,88].In addition to this, a few researchers also attempted to show effect of plasma proteins on 45S5 bioactive glass [89-91]. M.S. Bahniuket. al., recently provided a detail understanding of both the role of crystallinity and powder morphology on surface ions, and plasma protein adsorption by comparing crystalline and amorphous bioactive glass 45S5, in both melt-derived as well as sol-gel forms [92].

CHAPTER 3

3. Materials and Methods

3.1 Materials

The Precursors required for synthesis of bioactive glasses namely tetra -ethylorthosilicate (TEOS), Triethylphosphate (TEP), sodium acetate, calcium acetate, sodium nitrate and Calcium nitrate are procured from Sigma-Aldrich Company. The templates such as Gelatin type B from bovine skin (about 225 Bloom and molecular weight of 50 KDa) is obtained from Loba Chemie Pvt. Ltd. and highly polymerized fibrously prepared sodium salt form of CT-DNA is procured from Sigma-Aldrich company.

The others chemicals required for buffer solutions such as Tris(Hydroxymethyl)aminomethane Base(TRIZMA), Tris(Hydroxymethyl)aminomethane HCl (TRIMA) , Sodium dihydrogenphosphate and sodium hydrogenphosphate were
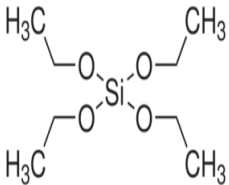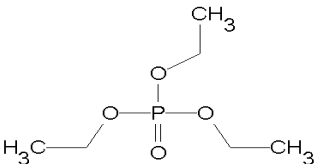
purchased from Sigma-Aldrich. Simulated body fluid (SBF, Henk's Balanced Salt solution) used for in vitro mineralization studies was obtained from Sigma-Aldrich company.

U$_2$OS, a human osteoblast-like osteosarcoma cell line (ATCC) was obtained from National Immunological Laboratory (NIA), Delhi. Dulbecco's modified eagle's medium of high glucose content (DMEM) was obtained from Sigma-Aldrich for the cell growth. The chemical required for the cytocompatability assay such as 3-(4,5-dimethylthiazol-2-yl)-2,5-diphenyltetrazolium bromide MTT, Triton-x HCl and Isopropanol was purchased from Sigma-Aldrich chemical company.

The solvents used are of AR grade 99.9% purity. Ethyl alcohol was obtained from Jiang Su Huaxi International Trade Co. LTD., acetone was bought from Central Drugs House (P) LTD. and glacial acetic acid was obtained from Sisco, Research laboratories Pvt. LTD.

Milli-Q water is used in all experiments. All other reagents used for experiments were of analytical reagent (AR) grade. The chemical structure of chemicals/biochemicals along with their manufacturing company used in this study is listed in the Table 3.1.

Table 3.1. List of Chemicals/Biochemicals used along with their chemical Structure.

S. No.	Name of the Chemicals/Biochemicals	Chemical Structure
1	Tetraethylorthosilicate(TEOS) Catalogue no. 333859 Sigma Aldrich	
2	Triethylphosphate(TEP) Catalogue no.538728 Sigma Aldrich	

3	Sodium acetate Catalogue no. 8750-250G Sigma Aldrich	
4	Calcium acetate Catalogue no.402850-100G Sigma Aldrich	
5.	Sodium nitrate Catalogue no. S5506 Sigma Aldrich	Na_2CO_3
6.	Calcium nitrate tetrahydrate Catalogue no. C1396 Sigma Aldrich	$CaNO_3.4H_2O$
7.	Acetone Catalogue no. 010512 Central Drugs House(P)LTD	
8.	Ethyl Alcohol AR 99.9% Jiang Su Huaxi International Trade Co. LTD Catalogue no.	
9.	Acetic Acid Catalogue no TT531762 Sisco, Research laboratories Pvt. LTD	
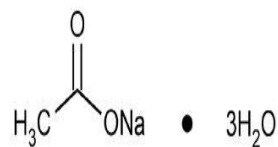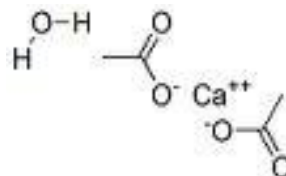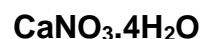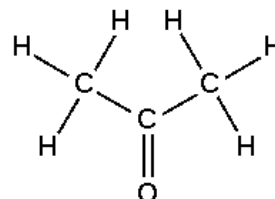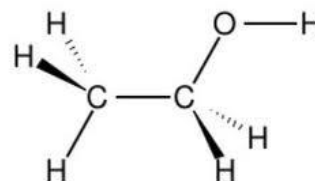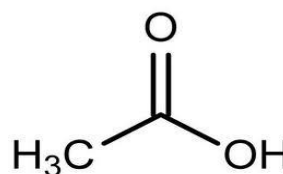
10.	Tris(Hydroxymethyl)aminomethane Base Catalogue no. 2044122 Sisco, Research laboratories Pvt. LTD	
11.	Tris(Hydroxymethyl)aminomethane HCl Catalogue no. 2044123 Sisco, Research laboratories Pvt. LTD	
12.	Calf Thymus DNA CAS 73049-39-5 Sigma	
13	Gelatin powder Catalogue no. 0392000500 Loba Chemie Pvt. Ltd	
14	Sodium dihydrogen phosphate	
15	Sodium hydrogen phosphate	
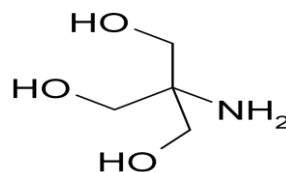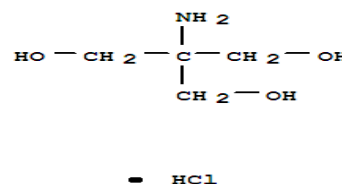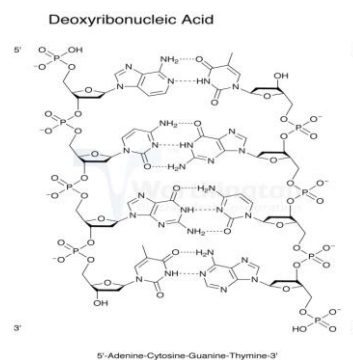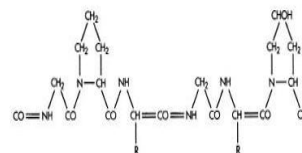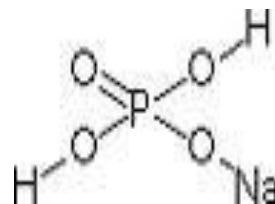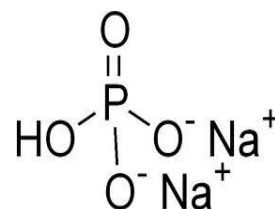
16.   Isopropanol
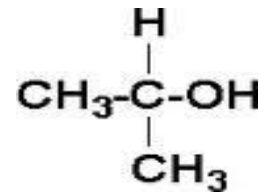
17.   3-(4,5-dimethylthiazol-2-yl)-2,5-diphenyltetrazolium bromide MTT,
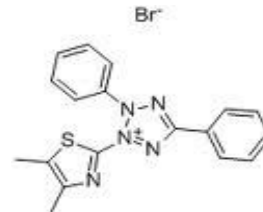
28.   Sodium dodecyl sulphonate

19.   Stimulated Body Fluid(SBF)
Henk's Balanced Salt solution
Catalogue no.H8264
Sigma Aldrich

20.   DMEM medium (DL-77)

3.2 Methods

3.2.1 Preparation of Buffer solutions

TRIZMA Buffer: An aqueous solution of 30mM tris(hydroxymethyl)aminomethane (TRIZMA) buffer at pH 8 was prepared by dissolving 1.82 g/L TrizmaHCl and 2.22 g/L Trizma base in milliQ water .

PBS Buffer: PBS buffer solution of pH 6.5 was obtained by mixing of 1.78 g/L of sodium dihydrogen phosphate and 0.27 g/L of sodium hydrogen phosphate salt solutions in milliQ water.

3.2.2 Preparation of Template solutions

CT-DNA: The required amount of DNA fibers was dissolved in 10 mL in 10 mM Trizma buffer solution at pH 8 in a 50 mL vial and kept in a orbital shaker (Thermo Scientific) at 180 to 220 rpm overnight at 37ºC.The concentration (in phosphate groups) of DNA stock solutions was measured spectropotometrically considering the molar extinction coefficient of the DNA base pairs to be equal to 6600 M^{-1} cm^{-1}. The ratio of absorbance 260 and 280 nm was found to be 1.8. Further, negligible absorbance was observed at 320 nm indicating the absence of protein contamination. Transition temperature T_m of CT-DNA was found to be 85ºC using Carry 100 concentration UV-visible spectrophotometer with temperature controller and found to be in good agreement with the information provided by Sigma (Figure 3.1). The B-form of DNA in solution was confirmed by the appearance of positive peak at 273 nm and negative peak at 245 nm using circular dichroism (Figure 3.2) (Jasco spectropolarimeter model 715). The CD spectrum was recorded between 220 and 325 nm.
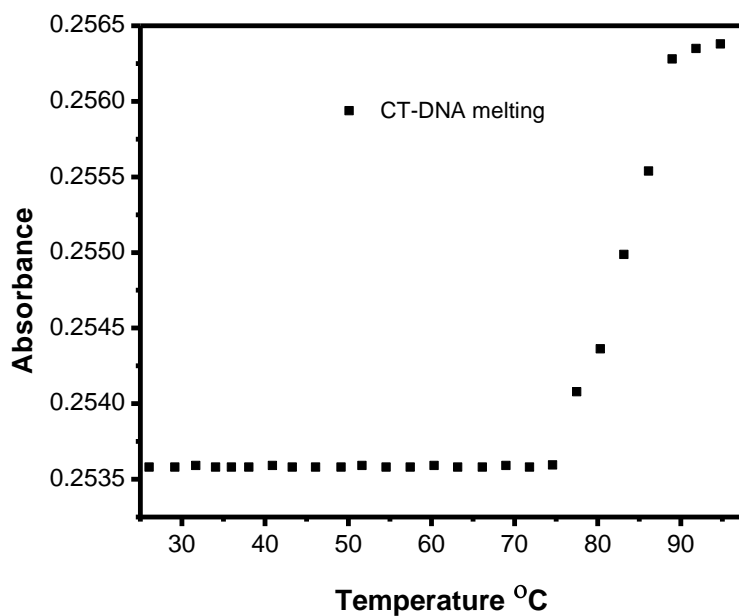
Fig. 3.1. UV melting transition of CT-DNA of 1 μM Concentration
with 10 mM tris buffer (pH 7)
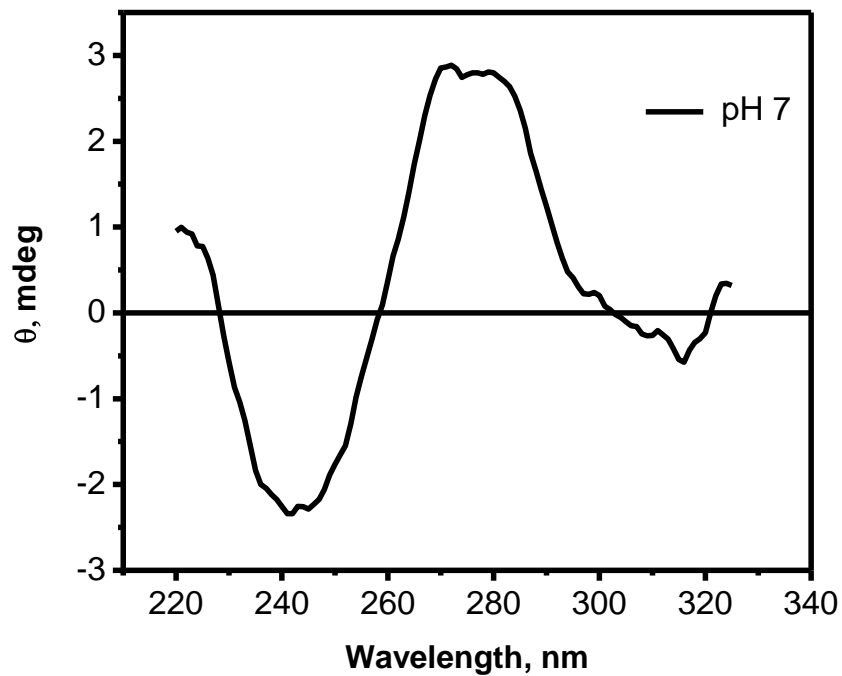
Fig. 3.2. CD-spectra of CT-DNA of 5 μM Concentration
with 10 mM tris buffer (pH 7)

Gelatinesolution: 1.2 g/L of gelatin solution was prepared by dissolving 1.2 g gelatin powder in 1 L of MilliQ water (1.2mg/mL).

3.2.3 Preparation of bioactive glass

The following three different routeswere used to synthesis 45S5 (45% SiO_2, 24.5% Na_2O, 24.4% CaO and 6% P_2O_5 (in wt. %) Bioactive glass:

a) Bio-inspired synthesis of 45S5 Bioactive glass using CT-DNA as template

Initially, the CT-DNA stock solution was mixed with 100 mL of TRIZMA buffer solution at pH 8 (10mM) in such a way to get 1000 µM of CT-DNA. The precursors namely 9.29 g of tetraethylorthosilicate, 1.0 g of triethylphosphate, 6.36 g of sodium acetate , 4.21 g of Calcium acetate were added slowly steadily one after another into the 100ml TRIZMA buffer containing CT-DNA. For mixing every precursor half an hour interval was given with constant stirring and left at 37⁰C with constant stirring in silicon oil bath for 24 hours. After 24 h a white colored precipitate was formed, centrifuged, washed with MilliQ water and dried at 40^0C in an air oven for 48 hours and preserved in air tight containers.

b) Bio-inspired synthesis of 45S5 Bioactive glass using gelatin as template

The 0.12g of gelatin stock solution was mixed with 100 mL of Trizma buffer solution at pH 8 (10mM) in such a way to get 1.2mg/ml concentration of Gelatin. The precursors namely 9.29 g of tetraethylorthosilicate, 1.0 g of triethylphosphate, 6.36 g of sodium acetate, and 4.21 g of calcium acetate were added slowly steadily one after another into the 100 mL Trizma buffer containing gelatin. After the addition of every precursor half an hour interval was given with constant stirring in silicon oil bath for 24 hours. After 24 hrs a white colored precipitate was formed, centrifuged, washed with MilliQ water and dried at 40^0C in an air oven for 48 hours and preserved in air tight containers.

c) Conventional Sol-Gel synthesis of 45S5 Bioactive glass using gelatin as template

Sol-gel synthesis of bioglass using gelatin as template was carried out by following Chitra et al. [93] with required modifications. To prepare the clear sol of gelatin (4g), tetraethyl orthosilicate(9.29g), triethylphosphate(1g), sodium nitrate (6.36g), calcium nitrate (4.21g) and acetic acid, the chemicals were dissolved in ethanol one by one with one hour interval for each addition of the chemical and stirred well at room temperature for 24 hours . The weight ratio of polymer to ethanol was maintained as 1:4 and ethanol to acetic Acid was 1:6. After 24 hours of continues stirring, the sol was aged for three days to evaporate the excess solvent and dried at 100 ^{0}C for 48 hours in an air oven. The excess gelatin present in the sample was removed by HCl treatment. For acid treatment, 48% HCl solution was prepared. 1 g of material was mixed with 100 ml of 48wt % HCl solution and heated at 95 ^{o}C for 24 hours. The resulting mixture was washed with acetone and dried at 80 ^{0}C for 36 h. After that material was calcinated at 450 ^{0}C for 4 h.

3.3 Characterizations Techniques

3.3.1 Fourier Transformation Infra Red Spectroscopy (FTIR)

Fourier transform infrared (FTIR) spectroscopy was performed on the bioactive glass samples before and after interaction with SBF solution at various time intervals using a NICOLET 380 FTIR spectrometer with an attenuated total reflection unit in evanescent mode. Dried samples were ground and mixed thoroughly with potassium bromide at the ratio of 1:100 (sample:KBr) and pelleted. The IR spectra of the pallets were then analyzed using NICOLET 380 FTIR operating at range 400-4000 of cm^{-1}.the spectrum was recorded at a resolution of $4cm^{-1.}$

3.3.2 X-Rays Diffraction (XRD) Analysis

For XRD analysis, powdered bio active glass samples of 500mg were used. On the other hand, for bioglass samples after interaction with SBF the Pallets were used to record XRD. XRD analysis on the glass samples were carried out to examine crystalline of the sample as well as the possible formation of Hydroxyapatite crystals at various immersion times in SBF using MiniFlex2 goniometer operating at voltage 30kV (15mA). XRD were recorded at 2θ angle range of 10 to 70 degrees and the process parameters were taken at step size 0.02 (2θ) and scan step time 4s.

3.3.3 Scanning Electron Microscopy (SEM) and Energy Dispersive X-Rays Spectroscopy (EDS)

The surface morphology of bioactive glass samples before and after interaction with SBF solution at various immersion times were characterized by thermal field emission gun scanning electron microscopy (FEI Quanta 200F). Before subjecting to SEM analysis, the samples were gold coated (5 nm thickness) and observed at accelerating voltage on of 12keV. Energy Dispersive X-Ray spectra (Kα line) (Oxford X-MAX) were collected at 20keV.

3.3.4 In Vitro Degradation Studies [97]

The degradation of various bioactive sample pellets were studied by immersing in phosphate buffer solution containing lysozyme (10,000U/mL) (PBS) at pH 7.2 and incubated at 37 ^{0}C for 7 days. Initially, the weights of various bioactive glass samples were noted as W_i. After 7 days of incubation with PBS buffer the glass samples were washed with deionised water to remove ions adsorbed on surface and lyophilized to dry. The dried weight of the corresponding samples were measured and noted as W_f. Using the following formula the degradation of the respective samples were calculated.

$$\overline{} \tag{1}$$

3.3.5 Density Measurement [97]

Densities of as prepared bioactive glass pellets were measured using DENVER Instrument SI-234 analytical balances equipped with density determination kit. Density measurements were carried out by using ethanol as the displacement medium. Before the experiment, the corresponding glass pellets were immersed in ethanol for 5 min and observed to cause no swelling or change in pore diameter. The density of the bioactive glass samples were calculated by using the equation given below:

$$\overline{} \tag{2}$$

Here;

Ma, Mass of the substance in Air

Me, Mass of the substance in solvent (ethanol)

ρ ,Density of the substance in g/cc

ρ_e ,Density of Ethanol=0.789 g/cc

3.3.6 Swelling Studies [97]

The Swelling studies on the bioglass samples were performed in PBS buffer of pH 7.2 at 37^0C in an incubator shaker. The known weight of respective bioglass pellet was placed in PBS for 1 hr. After one hour the glass pellet were removed from buffer solution. After removing the surface adsorbed water by filter paper, the pellets are weighed. Finally swelling ratio was calculated using equation 3.

$$\overline{\qquad}\qquad\qquad\qquad\qquad\qquad 3$$

Here;

W_w, is the weight of substance before placed in PBS

$W_{i,}$ is the weight of substance after removing from PBS

3.3.7 Assessment of bone bonding ability in SBF

The bone bonding ability of bioactive glass to host bone is revealed by the formation of a hydroxyl carbonate apatite (HCA) layer on the surface of the bio active glass ,either when implanted or placed in contact with biological fluid [94,95]. Hence, it can be preliminary assessed in vitro in SBF by monitoring the formation of HCA layer on its surface. As per the procedure described by Kokubo et al. [96], the powdered samples were made as pellets of equal size as well as shape of 13mm diameter and immersed in SBF solutions. The ratio of sample to SBF was maintained at 1mg into 1 ml SBF solution. Each sample was immersed in SBF for 1, 7 and 30 days in an ORBITEK incubator (Scigenics Biotech) at 37 ^{0}C under sterile conditions for the period of 1, 7 and 30 days. Once removed from the incubation solution, first the samples were rinsed gently with deionized water and then in acetone. Subsequently, the samples were dried in air at room temperature and stored in a dessicator for further characterizations. The sectioned samples were viewed under SEM and also subjected to EDX, XRD and FTIR analysis to examine the mineralization of hydroxyl apatite. Evolution of the SBF concentrations was monitored by means of pH value (Sigma instruments) caused by the

ion exchange processes between bioactive glass and the surrounding medium. The pH changes of the SBF before and after interaction with bioglass sample (BIS-BG-D) were measured and the correspondingly ions released (especially Ca and P) from glass sample were estimated by using inductively coupled plasma emission spectrometer (Jobin Yvon JY24).

3.3.8 Cell Studies

Biocompatibility of the human osteoblast cells were evaluated in two methods one is by growing the cells on to the pellet and the other method is called elution test method (ISO 10993-5).

Method I

Cell studies were carried out using U_2OS, a human osteoblast-like osteosarcoma cell line (ATCC). Cell lines were maintained in cell culture facility in DMEM medium of high glucose content with 10% heat-inactivated fetal bovine serum and 0.1% penicillin/streptomycin at 37ºC with 5% CO_2. Cells were detached from culture plate at 80-85% confluence and used for seeding on the bioglass pellets for investigating cytocompatibility of the biomaterial. Prior to cell seeding, the glass pellets were sterilized using UV treatment for 1 h and incubated with culture medium for 24 h at 37ºC with 5% CO_2 and 85% humidity. Then the culture medium was removed completely from the pellet. Cells were seeded drop wise onto the top of the pellet (1×10^5 cells/100µL of medium/pellet), which fully adsorbed the media, allowing the cells to distribute throughout the pellet. Subsequently, cell-seeded pellets were kept at 37ºC in a humidified incubator under standard culturing conditions for 4 h in order to allow the cells to attach the pellet. After each 4h, the pellets were fed additional culture medium and cells on the pellet were grown for 48h and subjected to MTT assay fro cell viability test as well as SEM analysis to examine morphology and spreading pattern of the cells.

MTT assay: The viability of cells grown on the pellet was determined using the colorimetric MTT (3-(4,5-dimethylthiazol-2yl)-2.5-diphenylterazolium bromide) assay. MTT assay measures the reduction of the tetrazolium component MTT by viable cells.

Therefore, the level of reduction of MTT into formazan crystals can reflect the level of cell metabolism. For the assay, cells were then seeded onto 96 well plates at a density of 10^4 cells/well and were incubated under standard culturing conditions. In order to carry out the assay initially, the 100 µL of 10% MTT reagent was added and covered the plate with foil by leaving some free space to get air and incubated for 2 h at 37^0C under cell culture conditions. After 2 h the plate was taken out and then added 100uL of MTT buffer (10% sodium dodecyl sulphonate, 0.1N HCl and isopropanol) by removing the cell culture medium and incubated for 20 min at cell culture conditions to dissolve formazan crystals. After incubation, plate was taken and read at 570 nm and 630 nm wavelengths using TECAN multimode plate reader.

Method II

In method II, the elution test method (ISO 10993-5) was adopted. Based on this method, extract from the pellets were prepared by incubating the pre-sterilized pellets in culture medium for 24 h and 37 ºC with agitation. The medium with bioglass extract was collected in falcon tube. Culture media of the seeded cells were replaced after 24h by the culture media containing bioglass extract. Cells were incubated on the extract for 24 h and 48 h and subjected to MTT-assay as explained in method I. In addition to this, cells were also observed under an optical microscope (NIKON ECLIPSE Ti-S) for visible signs of toxicity in response to the test. The cells cultured in DMEM medium was used as positive control. While 10% SDS treated DMEM medium was used as negative control.

All experiments were run with five samples and the data were represented as means ± SD.

CHAPTER 4

4. Results and Discussion

As already discussed in materials and methods 45S5 bioactive glass samples were synthesized in three different ways namely bio-inspired synthesis using CT-DNA / gelatin as template and sol-gel synthesis using gelatin as template. The resulted bioactive glass samples are named shortly for further discussion as follows: the glass synthesized using CT-DNA as template by bio-inspired rout is named as BIS-BG-D, when gelatin is used as template in the similar method, the sample is called as BIS-BG-G and the glass obtained by sol-gel method using gelatin as template is named SG-BG-G throughout this text.

4.1 Characterization of Bioactive glass samples

4.1.1 Fourier Transformation Infra-Red Spectroscopic (FTIR) Studies

FTIR spectra of CT-DNA sample and the bioglass sample BIS-BG-D is shown in Figure 4.1. From the figure it is evident that the spectrum of CT-DNA and BIS-BG-D are very different from each other except a few peaks correspond to the functional groups – O-H, and –N-H. In the spectrum of bioglass sample, the small sharp peak observed at 1715 cm^{-1} is attributed to –C=O stretching, whereas, a broad doublet at 1632 cm^{-1} and 1550 cm^{-1} are attributed to –O-H and -N-H deformations respectively. These peaks from the bioglass samples may be expected to arrive from water molecules, Trizma buffer as well as the template CT-DNA, since the drying process is below 100 ºC. The broad intense peak and small sharp peak at 1099 cm^{-1} and 788 cm^{-1} are attributed to Si-O-Si asymmetric stretching and bending vibrations respectively. The peak at 788 cm^{-1} is characteristic of ring structure of the glass matrix [98-100].

Figure 4.2 portrays FTIR spectra of gelatin and BIS-BG-G. In gelatin spectrum, two sharp small peaks at 1720 cm^{-1} and 1630 cm^{-1} are assigned to amide I (–C=O stretching) and amide II (N–H deformation and C–N stretching in –CO–NH– group bands) respectively. The small sharp peak at 1028 cm^{-1} could be due to skeletal vibrations of the molecules. The assignments of the observed bands for the above systems are made based on reported values for the various functional groups [101-103]. In the spectrum of the bioactive glass (BIS-BG-G), it is noteworthy that the characteristic bands of gelatin (amide I and amide II) are not appeared, which implies the glass sample is free from unreacted template molecules. Two small peaks observed in the spectrum of glass sample at 1653 cm^{-1} and 1561 cm^{-1} are expected from –O-H groups deformation of molecular water and –Si-OH group deformation respectively. The small shoulder at 940 cm^{-1} is attributed to –Si-OH (silanol) vibration and a sharp peak at 797 cm^{-1} is due to Si-O-Si bending vibrations of the glass sample [98-103].
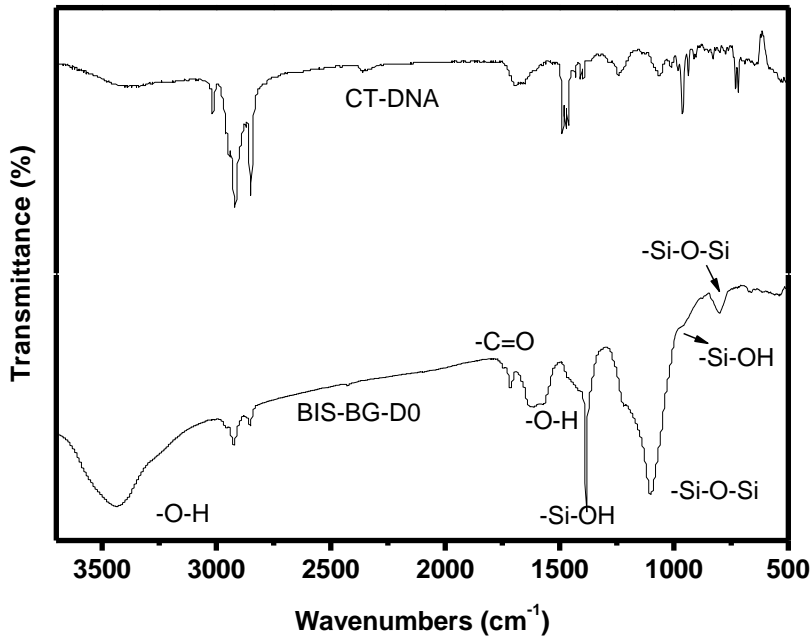
Fig.4.1. FTIR spectra of CT-DNA and BIS-BG-D.

The FTIR spectrum gelatin as well as sol-gel derived bioglass sample (SG-BG-G) are shown in Figure 4.3. The gelatin spectrum is already explained in Figure 4.2. Here again, it is pertinent to mention that the IR spectrum of SG-BG-G differs from gelatin spectrum. Similar to Figures 4.1, in Figure 4.2, the doublet at 1617 cm^{-1} and 1560 cm^{-1} is assigned to –O-H deformation and silanol group vibrations (-Si-OH). Whereas, a small shoulder at 1409 cm^{-1} is due to –N-H vibrations. The observed –N-H vibration may be arrived from the gelatin template. Intense broad band at the range of 1268-1021 cm^{-1} and sharp peak at 784 cm^{-1} are due to –Si-O-Si- vibrations of the glass sample [98-103]. It is noteworthy that, the observed vibrations of –O-H stretching (broad band in the region 3300-3700 cm^{-1}) and –O-H bending around 1600 cm^{-1} in all the three glass samples also indicate the presence of free water molecules, which may be trapped in the expected porous structure of the glass samples.
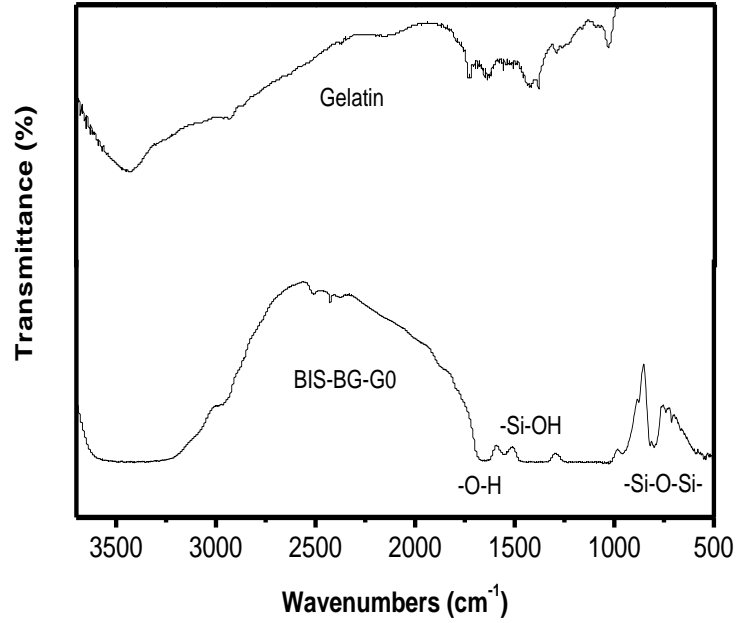
Fig. 4.2. FTIR spectra of gelatin and BIS-BG-G
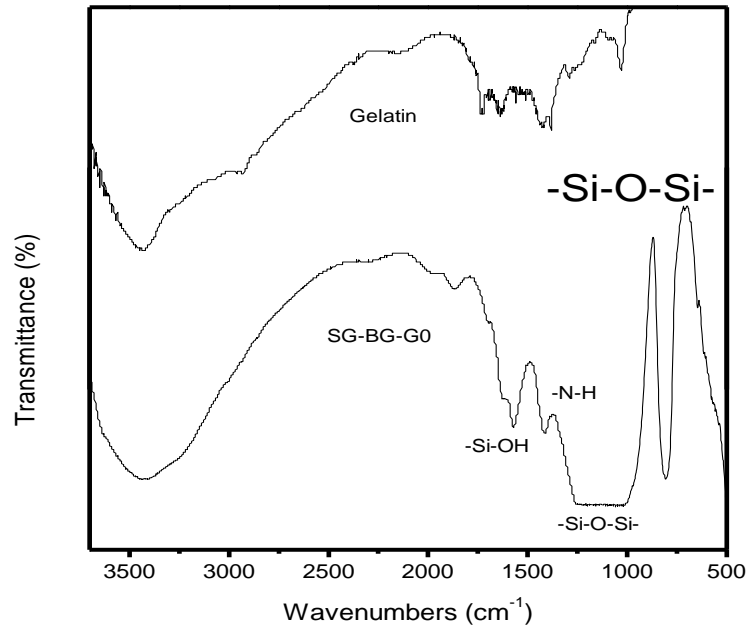
Fig. 4.3. FTIR spectra of gelatin and SG-BG-G

60

4.1.2 X-Ray Diffraction (XRD) Analysis

Figure 4.4 shows wide angle XRD pattern of BIS-BG-D. It is pertinent to recall that the bioglass synthesized by bio-inspired method using CT-DNA as template and dried below 100 ºC. The appearance of a broad band between 15 and 40 (2θ) with very few diffraction peaks at $2\theta=11.5^{o}$, 18.9^{o}, 22.5^{o}, 26.2^{o}, 29.6^{o} reveal the bioglass sample is mostly amorphous in state. The observed 2θ values are in close agreement with the $Na_2Ca_2Si_3O_9$ phase [104]. Thus the observed partial crystallization of as prepared 45S5 bioglass sample below 100 ºC is mainly due to CT-DNA molecule, which is known to be structure directing biomacromolecule [22]. It is expected that in the bio-inspired method, biomolecule, which is used as template as well as retain their originality. Additionally, it can induce crystallization of inorganic molecules from the solution phase at low temperature under atmospheric pressure [105-108].

The wide angle XRD pattern of BIS-BG-G is portrayed in Figure 4.5. Similar to BIS-BG-D (Figure 4.4) system here again, a broad band in the range of 15 and 40 (2θ) is observed along with a few sharp diffracted peaks at 29.28^{o}, 35.86^{o}, 39.42^{o}, $42,97^{o}$, 47.35^{o} and 48.45^{o} (2θ). The observed XRD pattern reveals that the system is in partially crystalline phase and the diffracted peaks are in good agreement with $Na_2Ca_2Si_3O_6$ phase [104]. Once again, as observed previously, gelatin molecule is expected to cause partial crystallinity of the inorganic phase at low temperature and pressure [105-108].

Figure 4.6 shows wide angle XRD pattern of SG-BG-G. The bioactive glass sample is synthesized by sol-gel method using gelatin as template. From this figure, it is evident that a broad band associated with amorphous silicate is observed between 15 and 40 (2θ) for the as prepared bioglass SG-BG-G. Interestingly, the diffracted peaks are not seen in this XRD pattern compared to BIS-BG-D and BIS-BG-G glass samples, which are prepared by bio-inspired route. Hence it is clear that the disappearance of diffraction peaks mainly due to sol-gel, the synthetic method, where the glass sample is calcined at 450ºC for 4 h. In sol-gel method, the template biomolecule gelatin is expected to degrade easily and loose its structure directing ability due to the absence of atmospheric conditions [105-108].
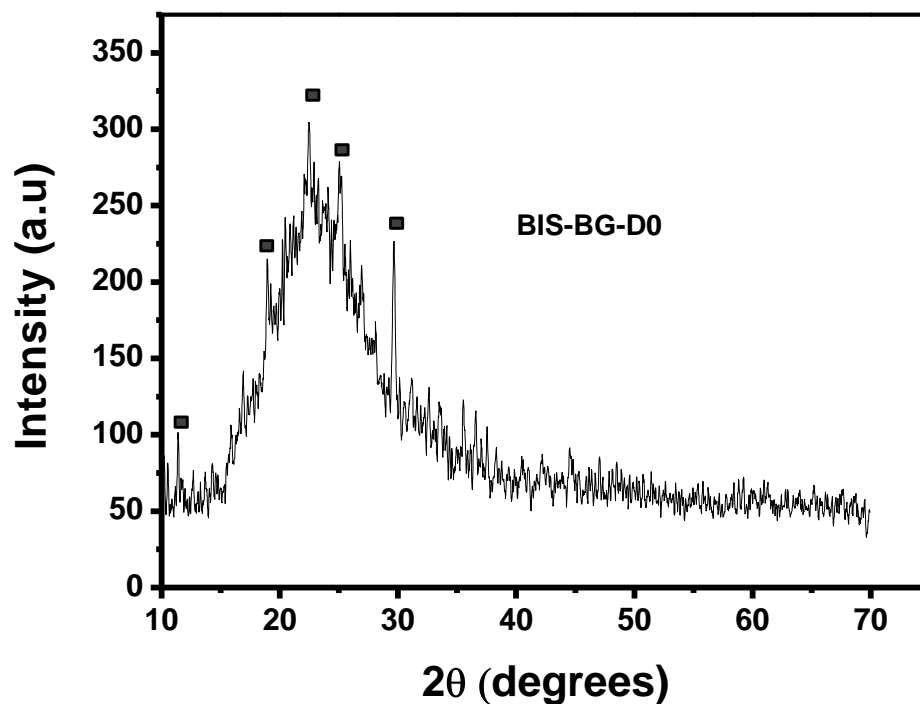
Fig. 4.4. Wide angle XRD pattern of as prepared BIS-BG-D.
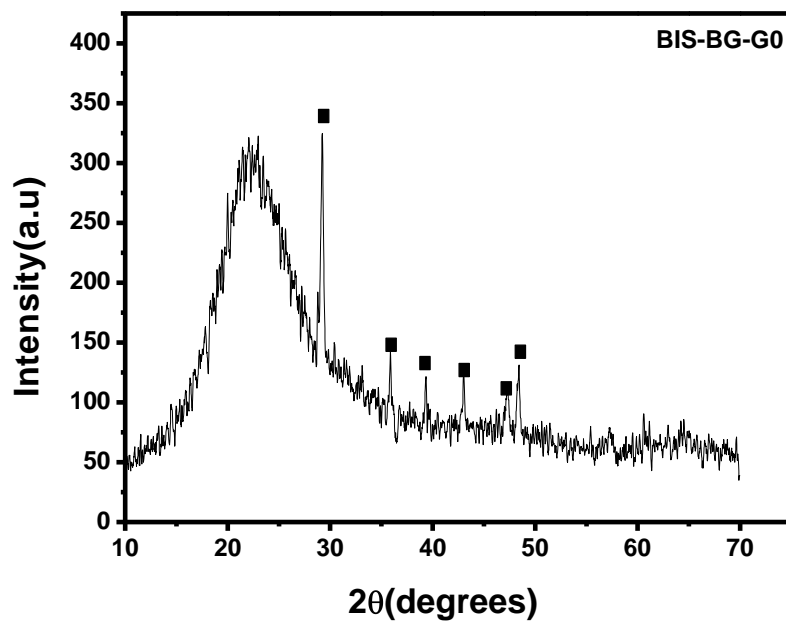
Fig. 4.5. Wide angle XRD pattern of as prepared BIS-BG-G.
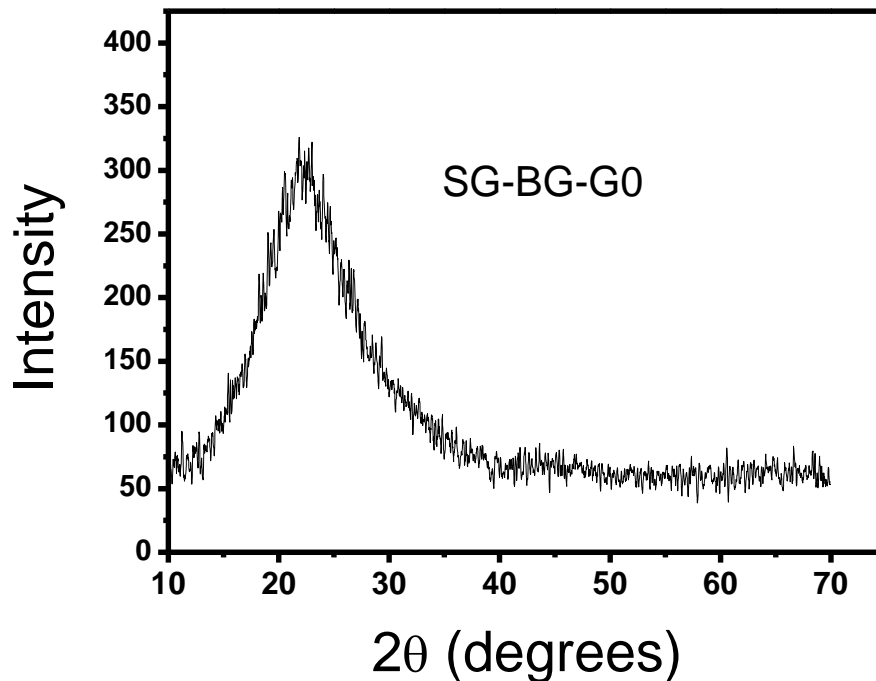
Fig. 4.6. Wide angle XRD pattern of as prepared SG-BG-G.

4.1.3 Scanning Electron Microscopy (SEM) and Energy Dispersive X-Ray Spectroscopy (EDS)

Figure 4.7 (a)-(c) shows SEM micrograph of BIS-BG-D bioglass sample of various magnifications. The BIS-BG-D particles are spherical shaped and size of the particle is approximately below 1 μm. interestingly, the morphology of bioglass sample is found to be highly porous with short range packing order. The EDS spectrum (Figure 4.7 (d)) of the bio active glass sample indicates the presence of elements such as Si, Ca, P, Na and O by showing the respective peaks in the spectrum. Based on the EDS spectrum the atomic ratio of Si:Na:Ca:P:O is observed to be 20.7:17.3:17.2:7.3:37.6, which is in good agreement with the calculated values (Please refer the table (e) given in Figure 4.7).
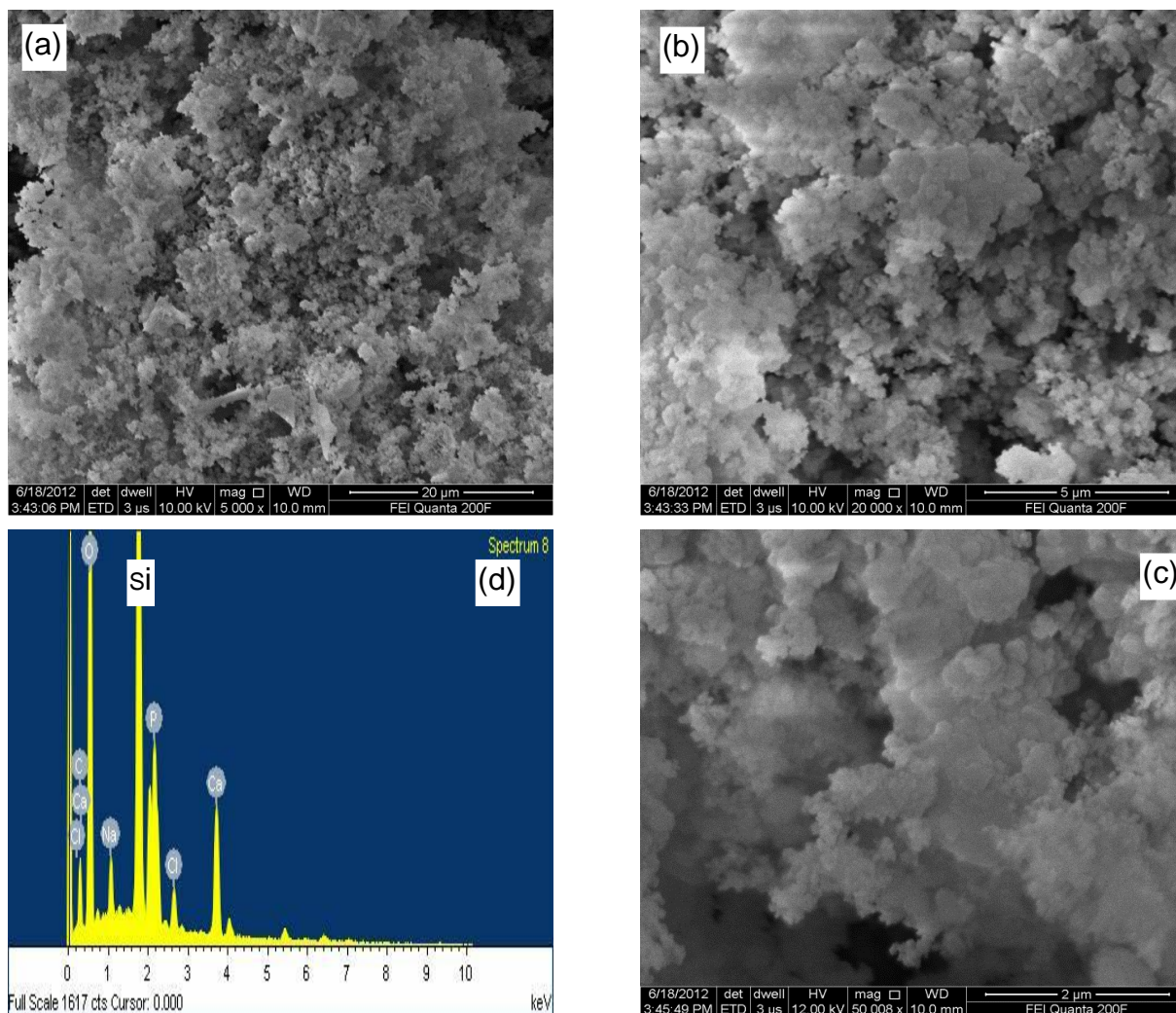
Elements	Atomic %	
	Observed	Calculated
Si	20.71	19.56
O	37.46	41,96
Na	17.31	17.56
Ca	17.22	15.12
P	07.30	05.77
Total	100.00	100.00

Fig.4.7. SEM (FESEM Quanta FEI 200) micrograph of BIS-BG-D at various magnifications (a) 5,000X, (b) 20,000X and (c) 50,000X. (d) EDS (Oxford X-MAX) spectra of BIS-BG-D showing the peaks of Si, Ca, Na, P and O. (e) A table showing calculated as well as observed atomic ratio of BIS-BG-D.

SEM micrograph of the bioactive glass sample BIS-BG-G is portrayed in Figure 4.8 (a) along with the EDS spectrum (Figure 4.8 (b)). The particle size of the glass sample is not very clear from the spectrum. On the other hand, the microstructure reveals porous morphology of short range order and the pores are of approximately in 4 µm size range. The EDS spectrum indicates the presence of the elements such as Si, Na, Ca, P, and O of ratio 22.1:14.5:16.3:7.2:39.8 respectively. The observed ratio of elements by EDS spectra is found to be in good agreement with the calculated values (Figure 4.8(c)).

(c)
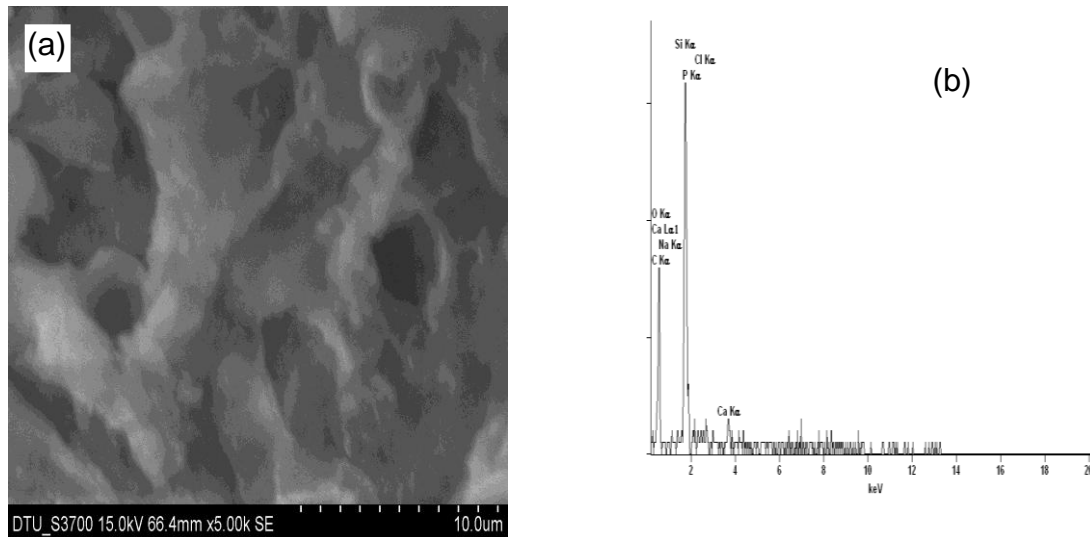
Elements	Atomic %	
	Observed	Calculated
Si	22.11	19.56
O	39.81	41,96
Na	14.55	17.56
Ca	16.32	15.12
P	7.21	05.77
Total	100.00	100.00

Fig.4.8. (a) SEM (HITACHI S-3700N) micrograph of BIS-BG-G. (b) EDS (Thermo scientific NORAN) spectra of BIS-BG-G showing the peaks of Si, Ca, Na, P and O (c) A table showing calculated as well as observed atomic ratio of BIS-BG-G.

Figure 4.9 (a) to (c) show the SEM micrograph of the glass sample SG-BG-G, the corresponding EDS spectrum and a table showing calculated and observed atomic percentage of the elements present in the sample. Based on the SEM micro graph of SG-BG-G, it is evident that the sample is mesoporous in nature. The sample is spherical shaped of range below 1 μm. The presence of elements Si, Na, Ca, P, and O are confirmed by EDS spectrum (Figure 4.9(b)) and the corresponding atomic percentage ratio of the elements are 22.3:15.4:18.2:8.1:46.0 respectively. Further, Table (c) of Figure 4.9 reveals calculated and observed atomic percentage ratio of elements of the glass sample is in close agreement.

(c)

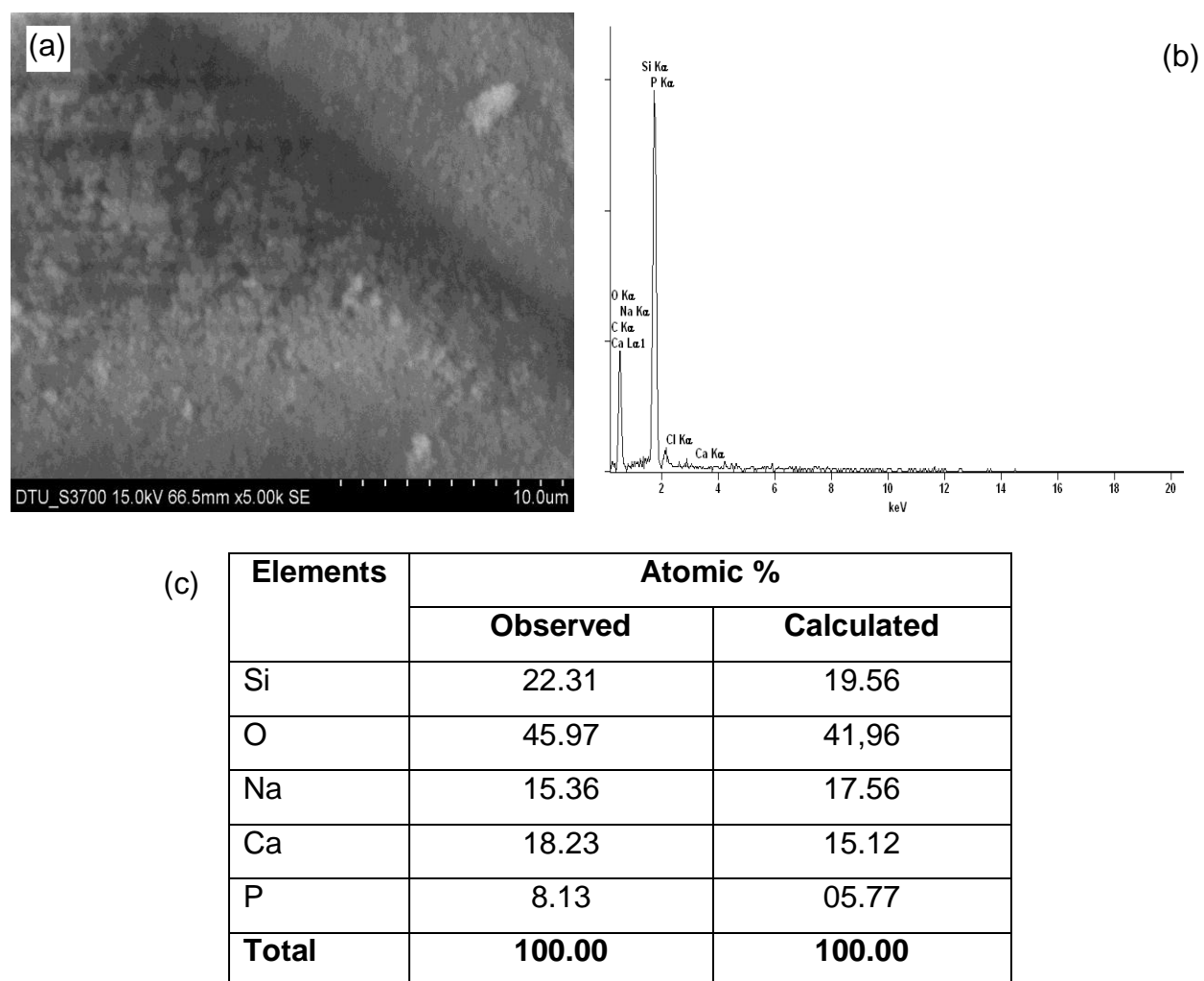| Elements	Atomic %	
	Observed	**Calculated**
Si	22.31	19.56
O	45.97	41,96
Na	15.36	17.56
Ca	18.23	15.12
P	8.13	05.77
Total	**100.00**	**100.00**

Fig. 4.9. (a) SEM (HITACHI S-3700N) micrograph of BIS-BG-G. (b) EDS (Thermo scientific NORAN) spectra of SG-BG-G showing the peaks of Si, Ca, Na, P and O and (c) a table showing calculated as well as observed atomic ratio of SG-BG-G.

Figure 4.10 shows the density of BIS-BG-D, BIS-BG-G and SG-BG-G glass samples along with their respective blank (glass prepared in the absence of template). In general, all blank samples show less density compared to in their respective bioglass samples prepared in the presence of template. The higher density of bioglass samples (BIS-BG-D and BIS-BG-G) prepared by bioinspired method in the presence of template DNA and gelatin are mainly due to their partial crystallinity (Figures 4.4 and 4.5) compared to their respective blank sample. In contrast, the highest density observed for the amorphous bioactive glass sample synthesized by sol-gel method using gelatin (SG-BG-G) compared to other glass samples could be attributed to the heat treatment of the sample at 450ºC. After the heat treatment the SG-BG-G sample must be free from molecular water and there is also more possibility for particulate close packing compared to BIS-BG-D and BIS-BG-G.

The swelling behavior of various bioactive glass samples BIS-BG-D, BIS-BG-G and SG-BG-G along with their respective blank (glass prepared in the absence of template) is portrayed in Figure 4.11. In general, swelling behavior of blank samples is more compared to the bioglass samples prepared in the presence of template. This shows in the presence of the template, association of the particles in the bioglass material is closer due to the chemical interaction between the organic and inorganic phase. Additionally, it is interesting to mention that the samples BIS-BG-D and BIS-BG-G show higher swelling behavior compared to SG-BG-G. This may be due to the difference in the synthetic route followed. It is pertinent to mention that Swelling studies were carried out to find possibility of infiltration of cells into the scaffolds, during in vitro cell culture. In general, higher the swelling character of the biomaterial higher infiltration of the cells is expected. Increase in the pore size due to the swelling allows cells to avail the maximum internal surface of the scaffolds. Samples higher degree of swelling will have larger surface area/volume ratio thus allowing the samples to have the maximum probability of cell growth. The increase in swelling also allows the samples to avail nutrients from the culture media more effectively. However, increase in swelling will also decrease the mechanical properties of the scaffold. Hence controlled swelling will be ideal for engineering applications [97].
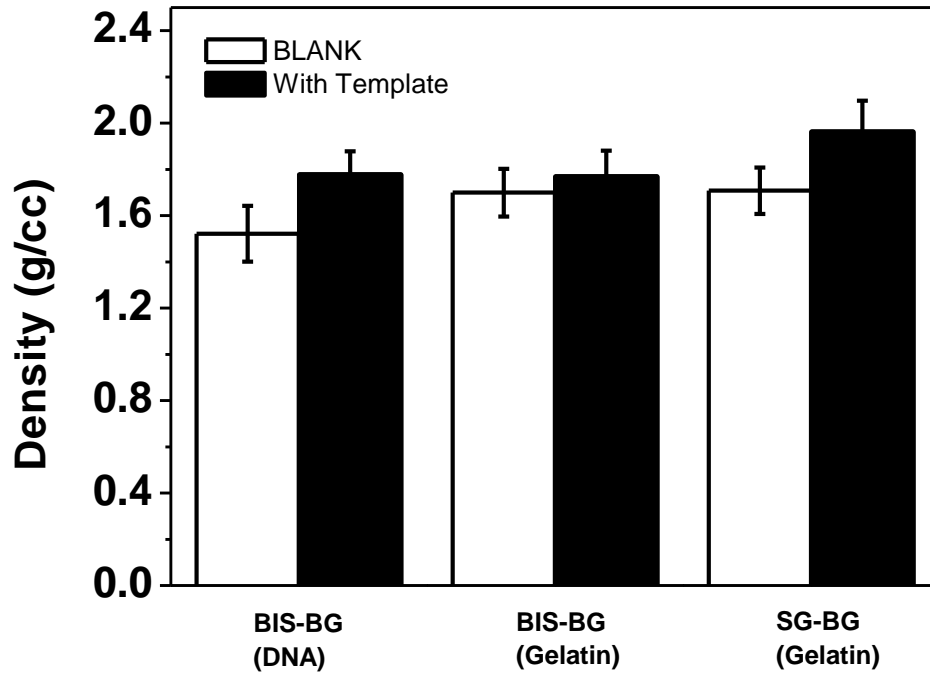
Fig.4.10. The density of various bioactive glass samples along with their respective blank (glass prepared in the absence of template).

Fig.4.11. The swelling behavior of various bioactive glass samples along with their respective blank (glass prepared in the absence of template).

In Figure 4.12 the degradation percentage of BIS-BG-D, BIS-BG-G and SG-BG-G glass samples along with their respective blank (glass prepared in the absence of template) are displayed. Generally, blank samples are found to degrade in phosphate buffer solution containing lysosyme in higher rate compared to the samples prepared in the presence of the template. Interestingly, the degradation of bioglass samples prepared in the presence of template show higher stability due to their lower swelling behavior (Figure 4.11) compared to their respective blank samples and may be attributed to the chemical interaction between the template and the inorganic phase. Additionally, bioglass synthesized by sol-gel method is found to show lowest degradation percentage compared to the bioglass samples prepared by bioinspired route. The observed the stability of SG-BG-G may be attributed to the calcination of the sample at 450 $^{\circ}$C compared to the samples which are dried below 100 $^{\circ}$C. The degradation is very important parameter for the scaffolds meant for tissue engineering application. This is because ideally the scaffolds should degrade as the formation of new tissue takes place [97].
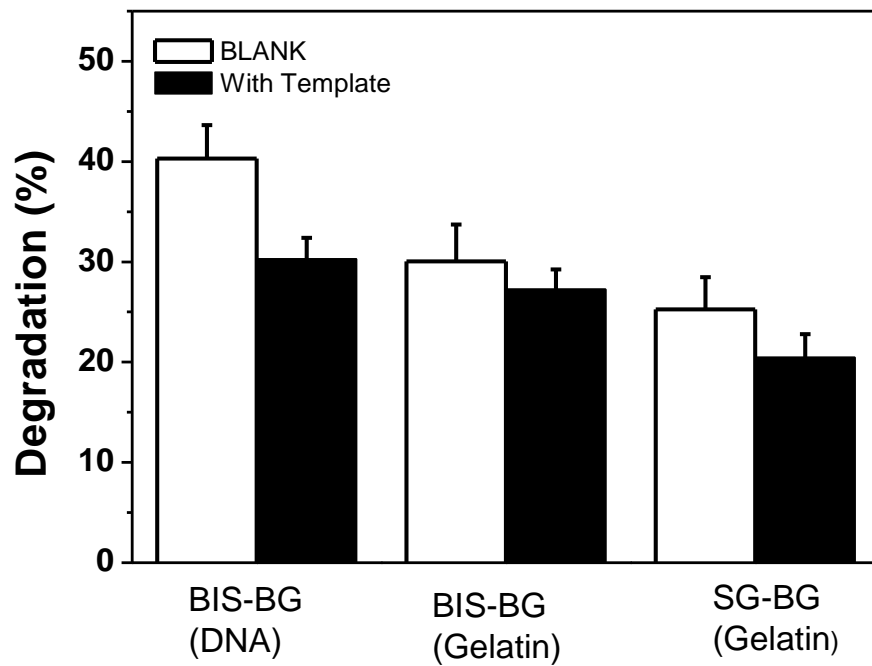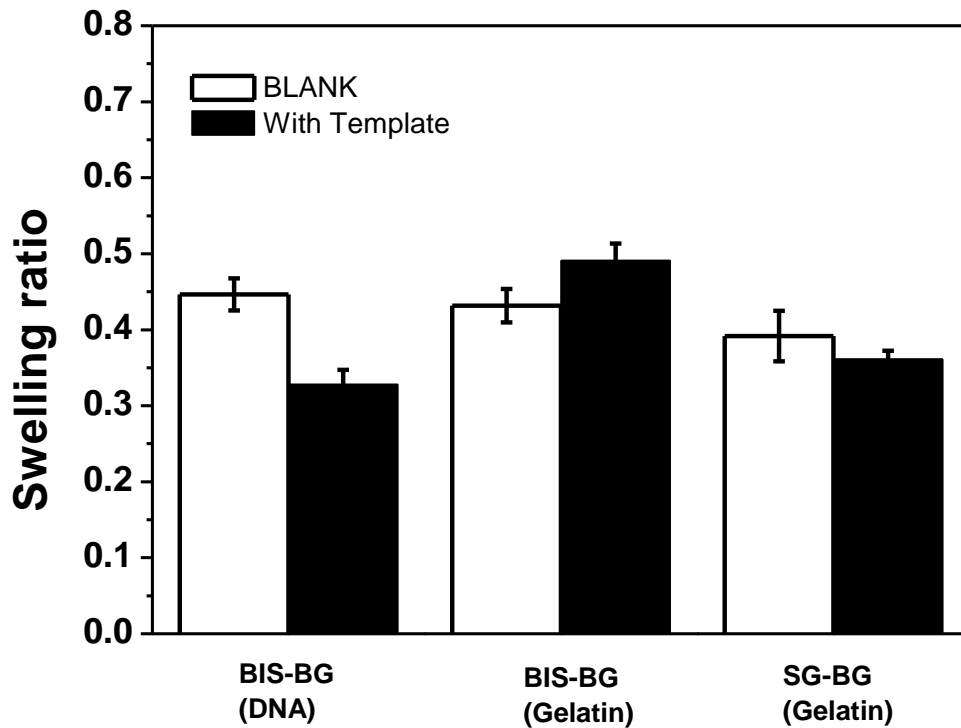

Fig.4.12. The swelling behavior of various bioactive glass samples along with their respective blank (glass prepared in the absence of template).

4.2 Assessment of in vitro bone bonding ability of bioglass samples

In vitro bone bonding ability of bioglass samples can be assessed by formation of hydroxyl carbonate apatite (HCA) on their surface, when they are immersed in simulated body fluid (SBF). Normally, the SBF solution contains ions namely Na^+, K^+, Mg^{2+}, Ca^{2+}, Cl^-, HCO_3^-, HPO_4^{2-} and SO_4 and the ion concentration is maintained nearly equal to those of human plasma [109]. It is well known from literature that the essential requirement for an artificial material to bond to living bone is the formation of bone like apatite on its surface, when implanted in the defective place and that this in vivo apatite formation can be reproduced in simulated body fluid. This indicates that in vivo bone bonding activity of a biomaterial can be predicted from the rate of apatite formation on its surface in SBF [109]. Based on this a number of researchers carried out in vitro bioactivity of biomaterials by examining the formation of apatite on their surface by immersing the biomaterials as pellets in SBF at various time intervals [85,86,91,93,96]. In this investigation, we have carried out the in vitro bone bonding activity of as synthesized bioactive glass materials (BIS-BG-D, BIS-BG-G and SG-BG-G) by immersing them in SBF at various time intervals (0, 1, 3, 7, 14 and 30 days) in the form of pellets of size 13 mm diameter. After the immersing the bioglass samples at required time, their surface is tested for the formation of apatite by various techniques such as FTIR, SEM and XRD.

4.3 Fourier Transform Infra Red Spectroscopic (FTIR) Studies

Figure 4.13 shows the FTIR spectra of BIS-BG-D before and after interaction with SBF at various immersion timings. As prepared glass sample shows the vibrational modes corresponds to the phosphate and silicate groups. Interestingly, after immersing the glass samples into the SBF, appearance of new peaks corresponds to phosphate and carbonate group (such as 1109, 965, 594, 556 and 507 cm^{-1}) after interaction with SBF at various time intervals indicate the formation of apatite phase. It is also note worthy that with increase in the interaction time of glass sample with SBF, the intensity of the phosphate peaks are observed to increase. The observed in vitro bioactivity by analyzing phosphate absorption bands in the spectra were in good agreement with other researchers [85,86,91,93,96] confirming the formation of an apatite-like phase. In

addition to the phosphate peak absorption, bands are also at 1489, 1414 and 864 cm^{-1}, which are attributed to carbonate group absorption bands.

Fig. 4.13. FTIR spectra of bioglass BIS-BG-D before and after interaction with SBF at various immersion timings. The presences of phosphate and carbonate bands are marked in the spectra.

The FTIR spectra of BIS-BG-G sample before and after interaction with SBF at various immersion timings (0, 1,7,10 days) are shown in Figure 4.14. Similar to the FTIR spectra of BIS-BG-D (Figure 4.13), we observe new peaks at 1109, 965, 594, 556 and 507 cm^{-1}, which correspond to phosphate and carbonate group vibrations with increasing the time. Additionally, the presence of carbonate groups can be identified with the presence of bands at 1489, 1414 and 864 cm^{-1}.

Fig. 4.14. FTIR spectra of bioglass BIS-BG-G before and after interaction with SBF at various immersion timings. The presences of phosphate and carbonate bands are marked in the spectra.

The FTIR spectra of BIS-BG-G before and after interaction with SBF at various time intervals (0,1,7,30 days) are portrayed in Figure 4.14. In comparison to the FTIR spectrum of bioglass at 0 day, the interaction with SBF leads to the significant changes in the FTIR spectra of the glass sample by the appearance of new peaks at 1109, 965, 594, 556 and 507 cm^{-1}, which correspond to phosphate group vibrations. In comparison with Figures 4.13 and 4.14, the spectra of SG-BG-G reveals absence of carbonate bands due to the calcination of the sample.
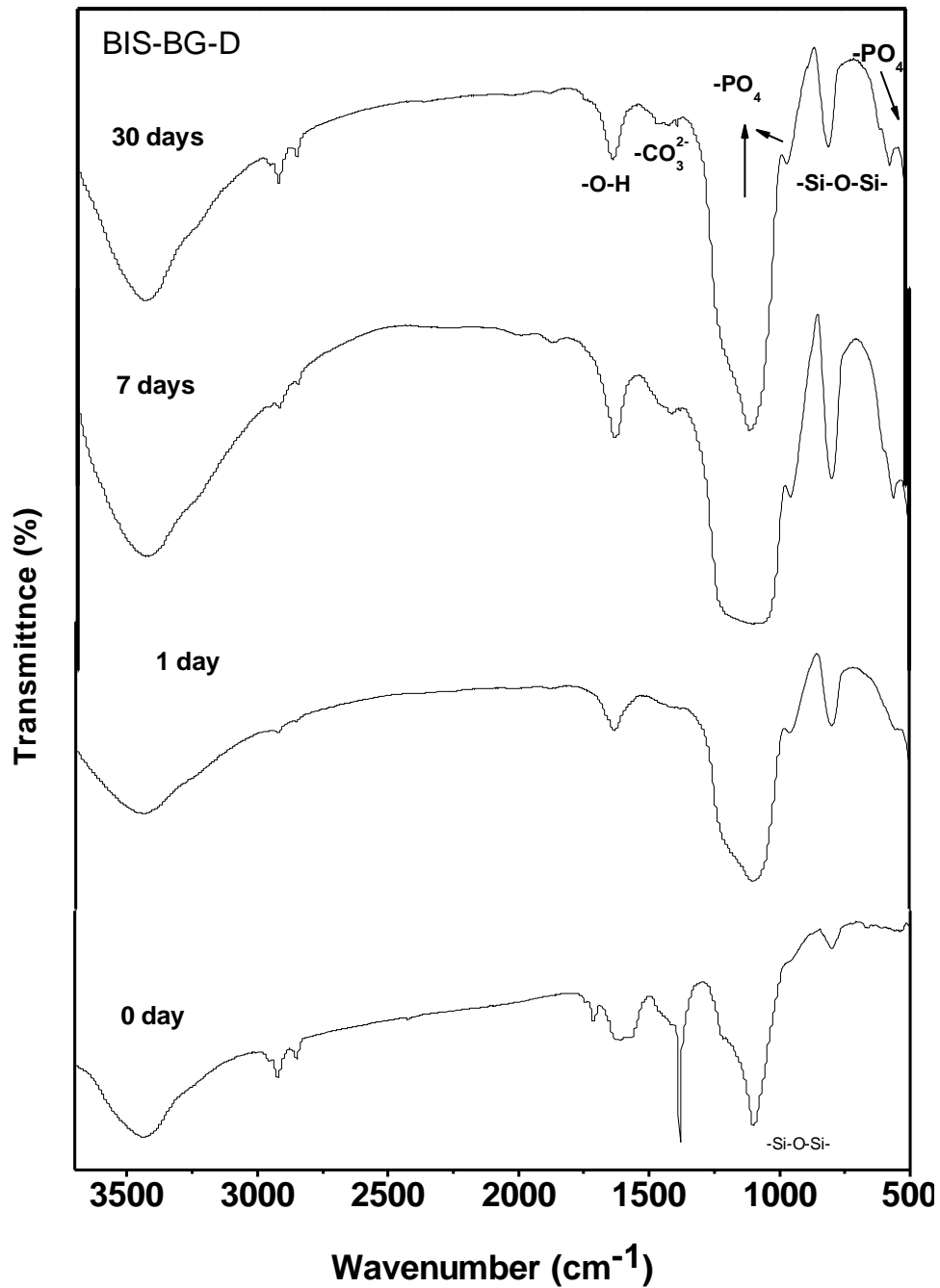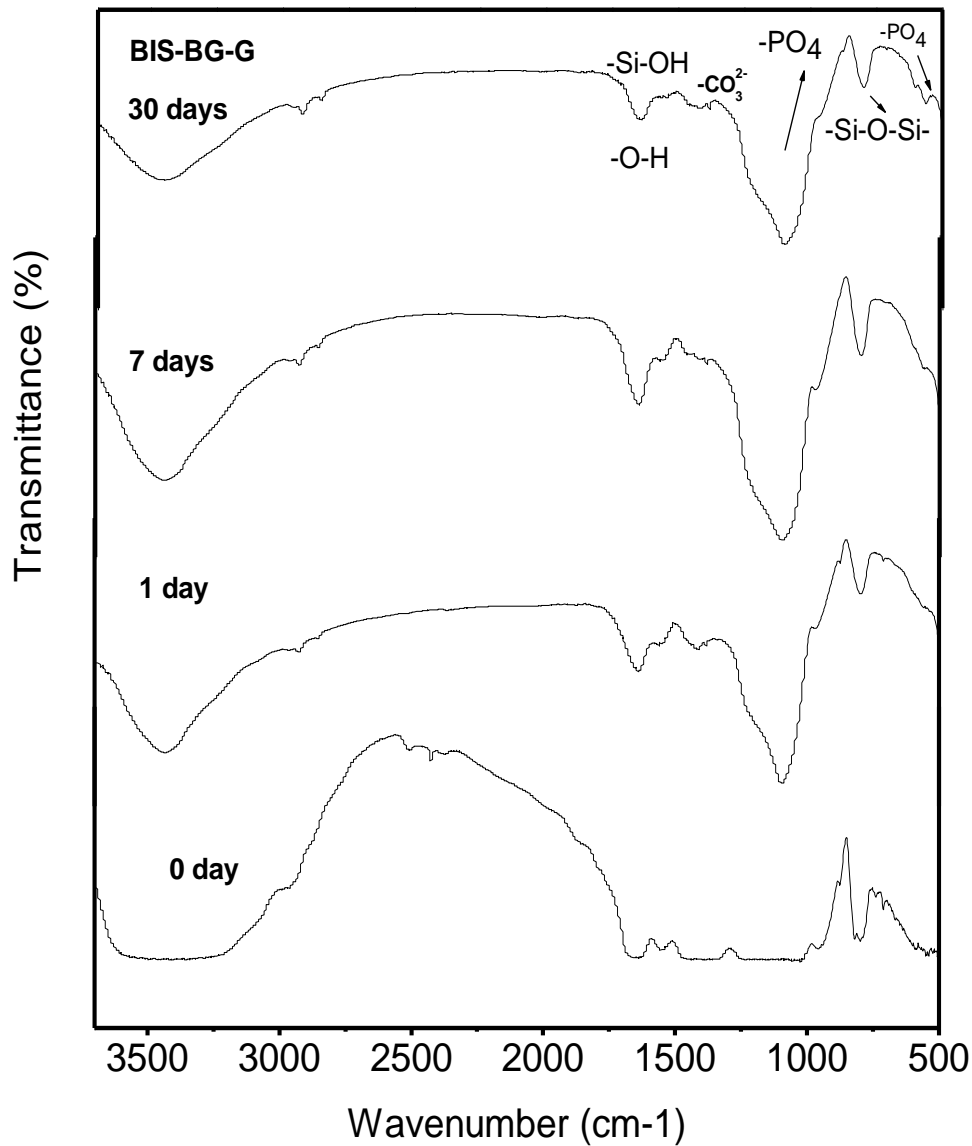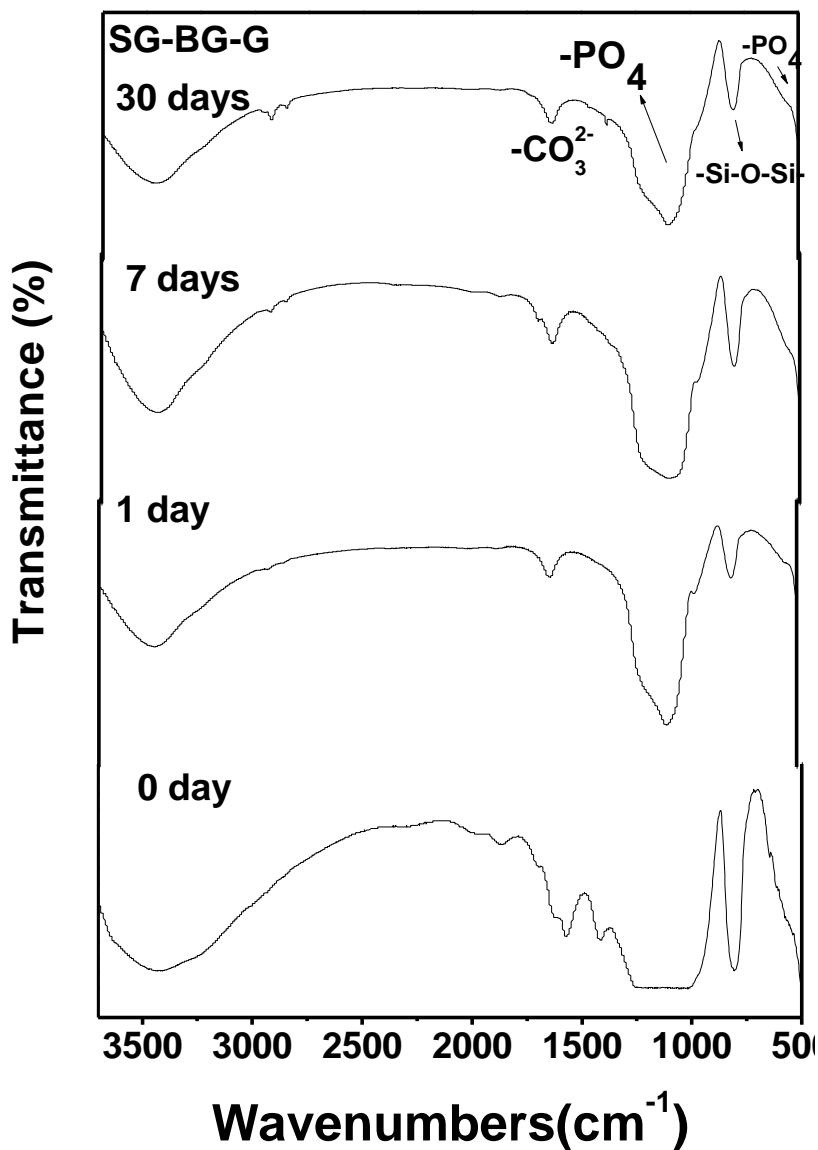

Fig. 4.15. FTIR spectra of bioglass SG-BG-G before and after interaction with SBF at various immersion timings. The presence of phosphate and carbonate bands is marked in the spectra.

4.4 X-ray Diffraction (XRD) Analysis

Wide angle XRD spectra of BIS-BG-D before and after interaction with SBF at various immersion timings are shown in Figure 4.16. The XRD spectrum of as prepared sample BIS-BG-D has been discussed in the earlier section (Figure 4.4). Interestingly, after one day interaction with SBF, the disappearance of diffracted peaks can be observed in the XRD spectrum. The observed disappearance of diffracted peaks after one day indicates change in the structure or rearrangement of local structure in the as prepared sample. It is also pertinent to recall that, the phosphate as well as carbonate vibrational modes are observed on the surface of the glass sample after interaction with SBF (Figure4.13). In addition to this, based on literature, the observed vibrational modes are corresponds to the hydroxyl carbonate apatite [85,86,91,93,96]. With an increase of soaking time, the interaction of bioactive glass sample with SBF becomes more severe, which leads to the formation of amorphous hydroxy apatite phase

Figure 4.17 shows wide angle XRD spectra of bioglass BIS-BG-G before and after interaction with SBF at various interaction timings. Similar to Figure 4.16, here again, the initial phase found in the as prepared glass sample is found to disappear after interaction with SBF may be indicating the deposition of amorphous hydroxyl apatite phase on the surface.

The wide angle XRD of as prepared SG-BG-G glass sample is found to be amorphous (Figure 4.18). Similar to the systems BIS-BG-D and BIS-BG-G, in the XRD of the bioglass SG-BG-G sample, the amorphous nature of the sample surface is retained after interaction with SBF.

Based on the above XRD and FTIR results, we suggest that nature of local structural changes on the as prepared bioglass sample upon soaking in the SBF. On one hand, the FTIR spectra reveals that the formation of HCA phase with sufficient soaking in the SBF. On the other hand, the XRD pattern provides the information about the nature of the phase formation, i.e. crystalline or amorphous. The present results confirm that the formed apatite phase remains in the amorphous state.

In this context, it is worth to consider the recent work on sol-gel prepared bioactive alkali modified calcium silicate glasses [110]. It has been observed that the

crystallization of amorphous HCA layer is strongly influenced by the textural properties by comparing the XRD patterns. The crystallization of apatite rich phase is hindered by other kinetic parameters, which could be compensated by the presence of CaO. It is known that this phase is extremely soluble and effectively increase the actual content of the phosphorous into the super saturation in the external physiological environment.

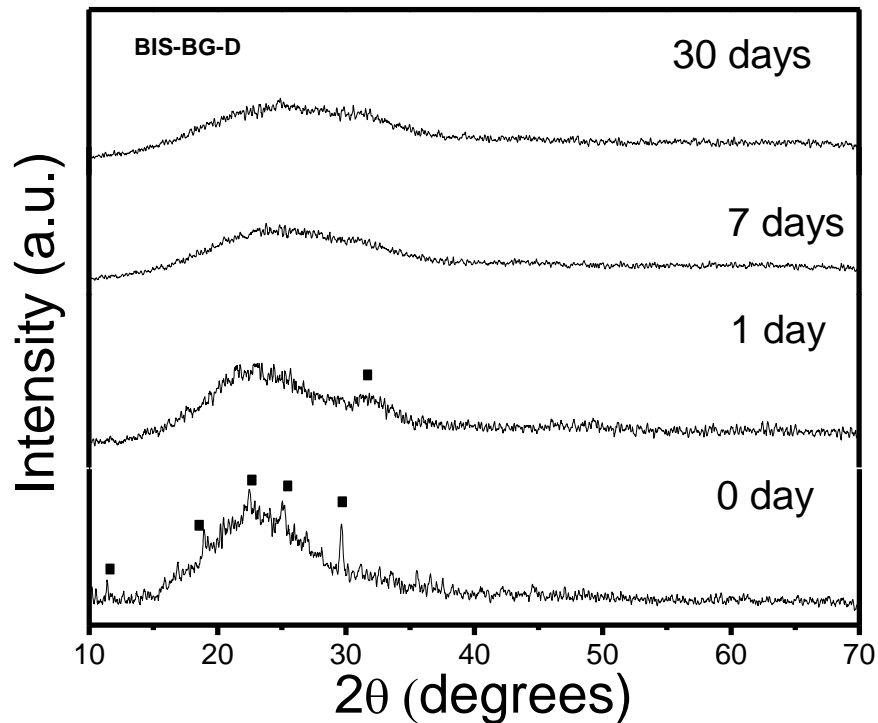**Fig. 4.16. Wide angle XRD spectra of bioglass BIS-BG-D before and after interaction with SBF at various immersion timings**.
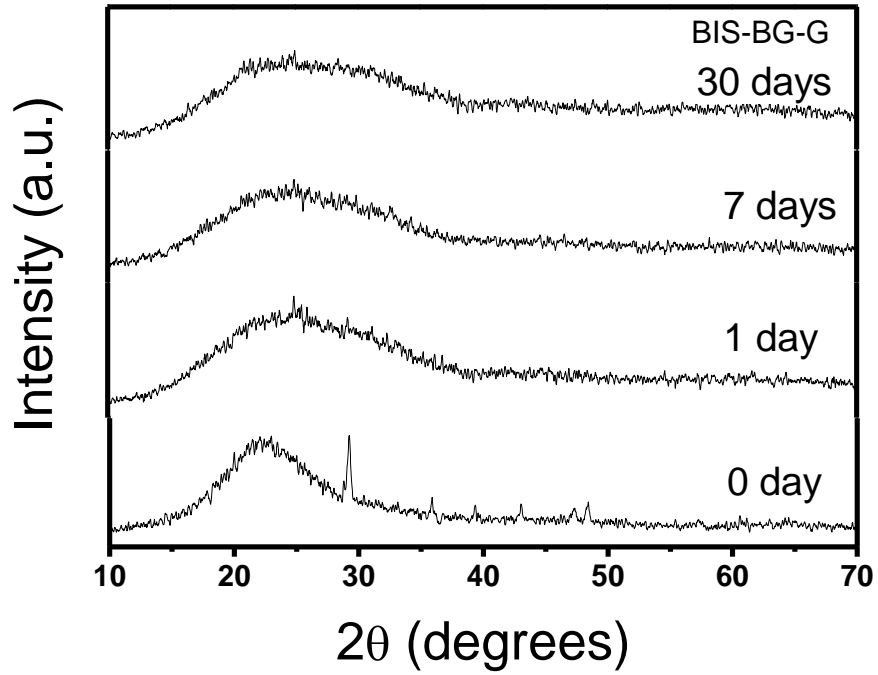
Fig.4.17. Wide angle XRD spectra of bioglass BIS-BG-G before and after interaction with SBF at various immersion timings
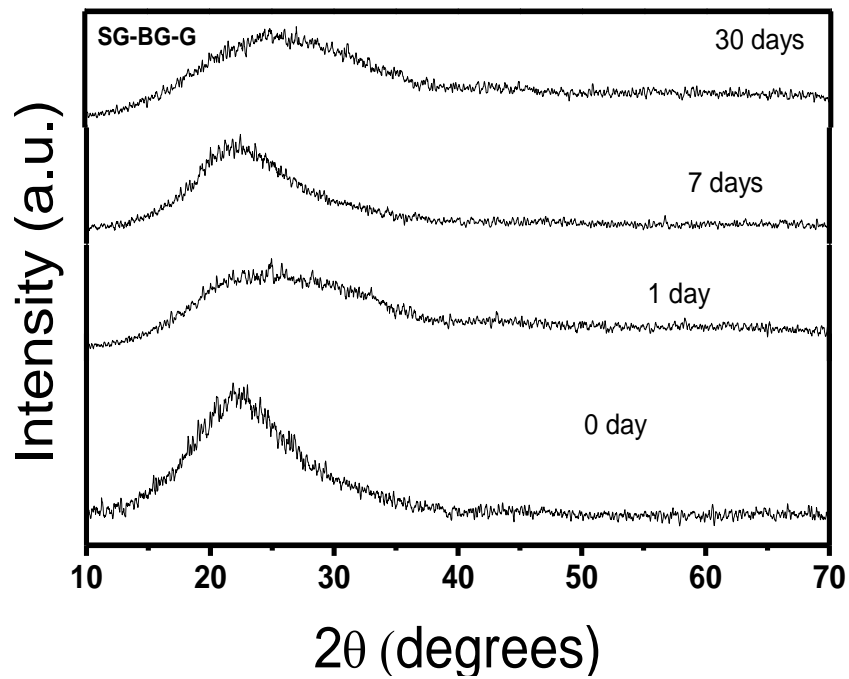

Fig.4.18. Wide angle XRD spectra of bioglass SG-BG-G before and after interaction with SBF at various immersion timings

4.5 Scanning Electron Microscopy (SEM) and Energy Dispersive X-Ray Spectroscopy (EDS)

Figure 4.19 Portrays SEM (FESEM Quanta FEI 200) micrographs of bioglass (BIS-BG-D) surface morphology after (a) 0 day (b) 1 day (c) 7 days and (d) 30 days interaction with SBF at 40,000X magnification. At 0 day of interaction with SBF (Figure4.19 (a)), the bioactive glass surface looks clean and shows mesoporous microstructure as explained earlier (Figure 4.7 (a)-(c)). From the figure it is interesting to note the growth of hydroxy apatite deposition on the glass surface is obvious after 1 day interaction time with SBF. Further, it is pertinent to mention that the apatite deposition increases rapidly with increase in interaction time with SBF (Figure 4.19 (c) and (d)). The corresponding EDS (Oxford X-MAX) spectra of the bioglass sample are displayed in Figure 4.20 (a)-(d) before and after interaction with SBF solution. A bar chart showing the observed atomic percentage of Ca and P by EDS spectra before and after interaction with EDS is also portrayed in Figure 4.20. It is worth to note that atomic percentage of Ca and P is found to increase with increase of interaction time of bioglass sample with SBF solution. The SEM and EDX analysis confirm the precipitation of hydroxy apatite on the bioglass surface, when it is in contact with the SBF solution. These results are in line with FTIR (Figure 4.13) and XRD analysis (Figure 4.16) of BIS-BG-D sample after interaction with SBF.
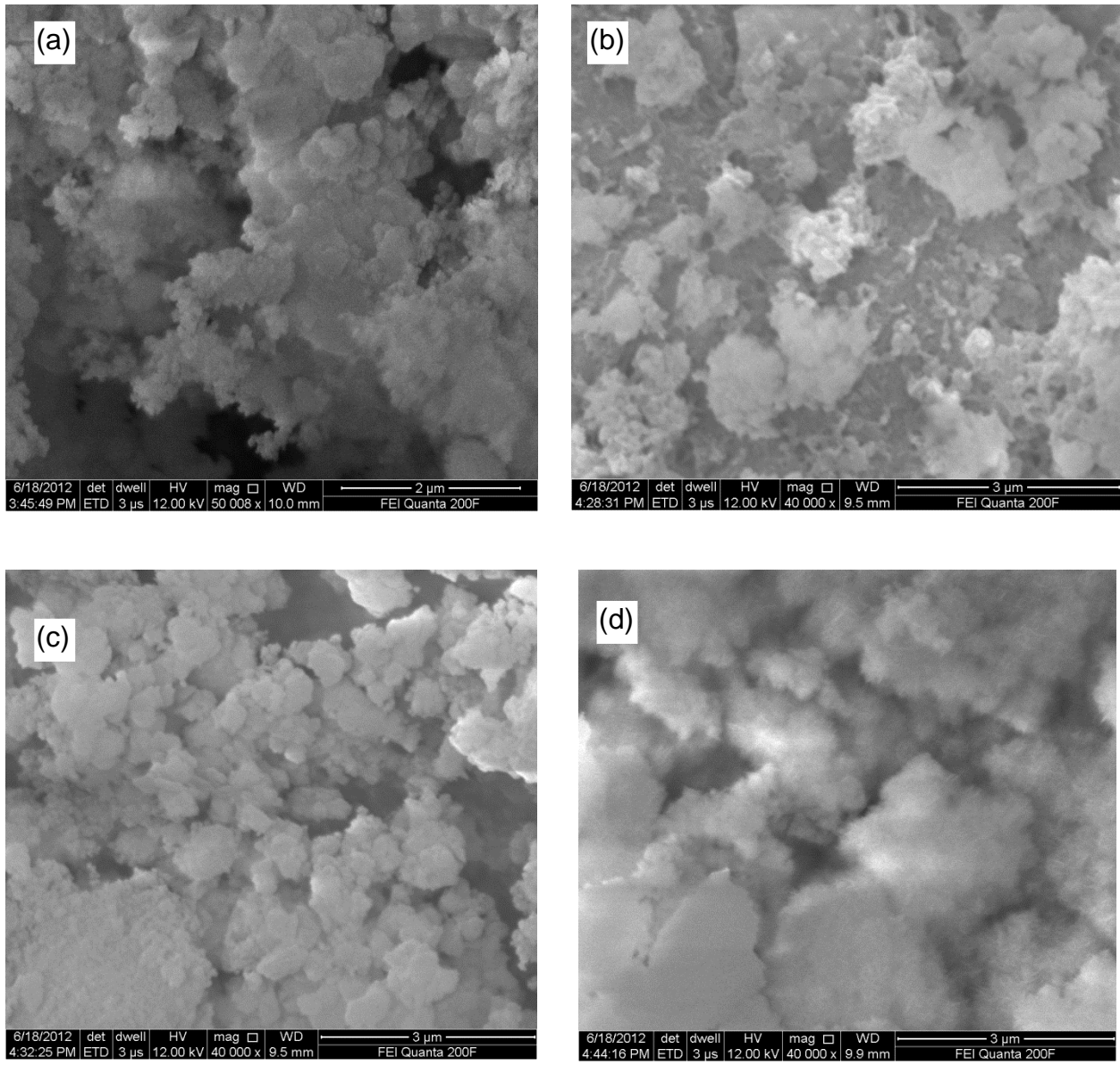
Fig. 4.19. SEM (FESEM Quanta FEI 200) micrographs showing surface morphology of bioglass BIS-BG-D after (a) 0 day (b) 1 day (c) 7 days and (d) 30 days interaction with SBF at 40,000X magnification.
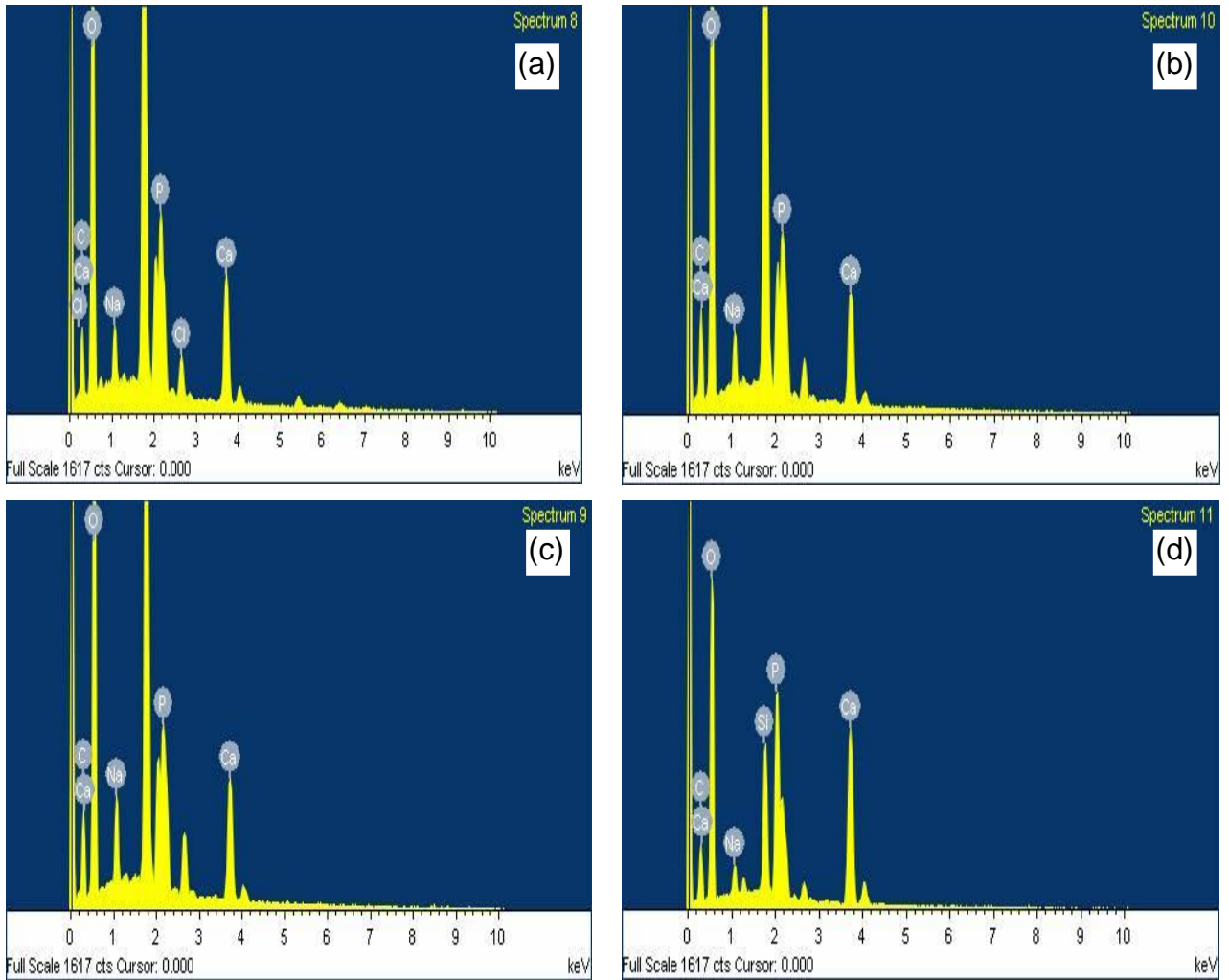
Fig. 4.20. EDS (Oxford X-MAX) spectra of the bioglass sample (BIS-BG-D) after (a) 0 day (b) 1 day (c) 7 days and (d) 30 days interaction with SBF.
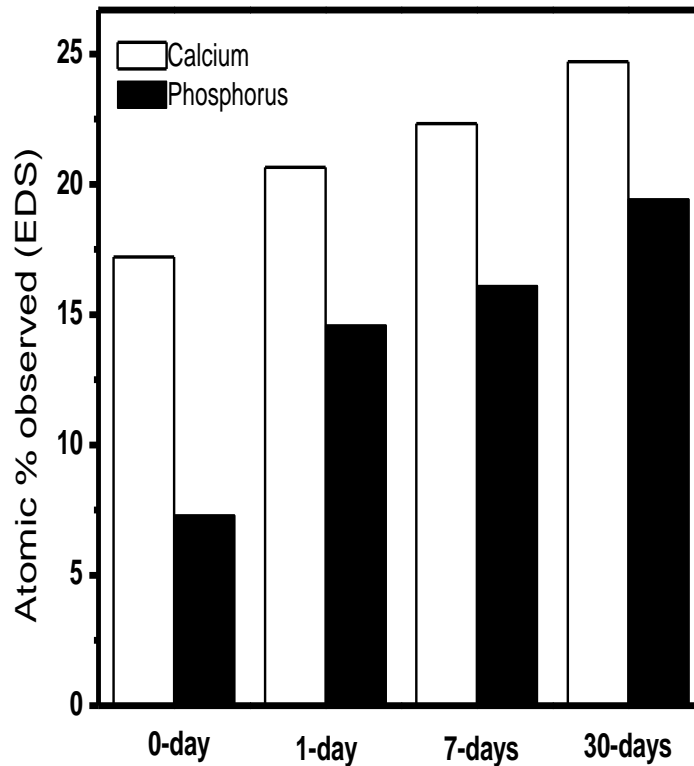
Fig.4.21. The atomic % of calcium and phosphorous of BIS-BG-D surface before and after exposing to SBF solution (observed by EDS).

SEM (HITACHI S-3700N) micrographs of bioglass (BIS-BG-G) surface morphology before interaction with SBF (Figure 4.22 (a)) show clear surface (which is already explain in detail (Figure 4.8)) compared to the bioglass morphology, after interaction with SBF for 30 days (Figure 4.22(c)). More interestingly, the EDS spectrum of the glass sample after interaction with SBF shows Ca and P peaks indicating the deposition of hydroxy apatite. These results are in good agreement with the corresponding FITR (Figure 4.14) as well as XRD (Figure 4.17) analysis.
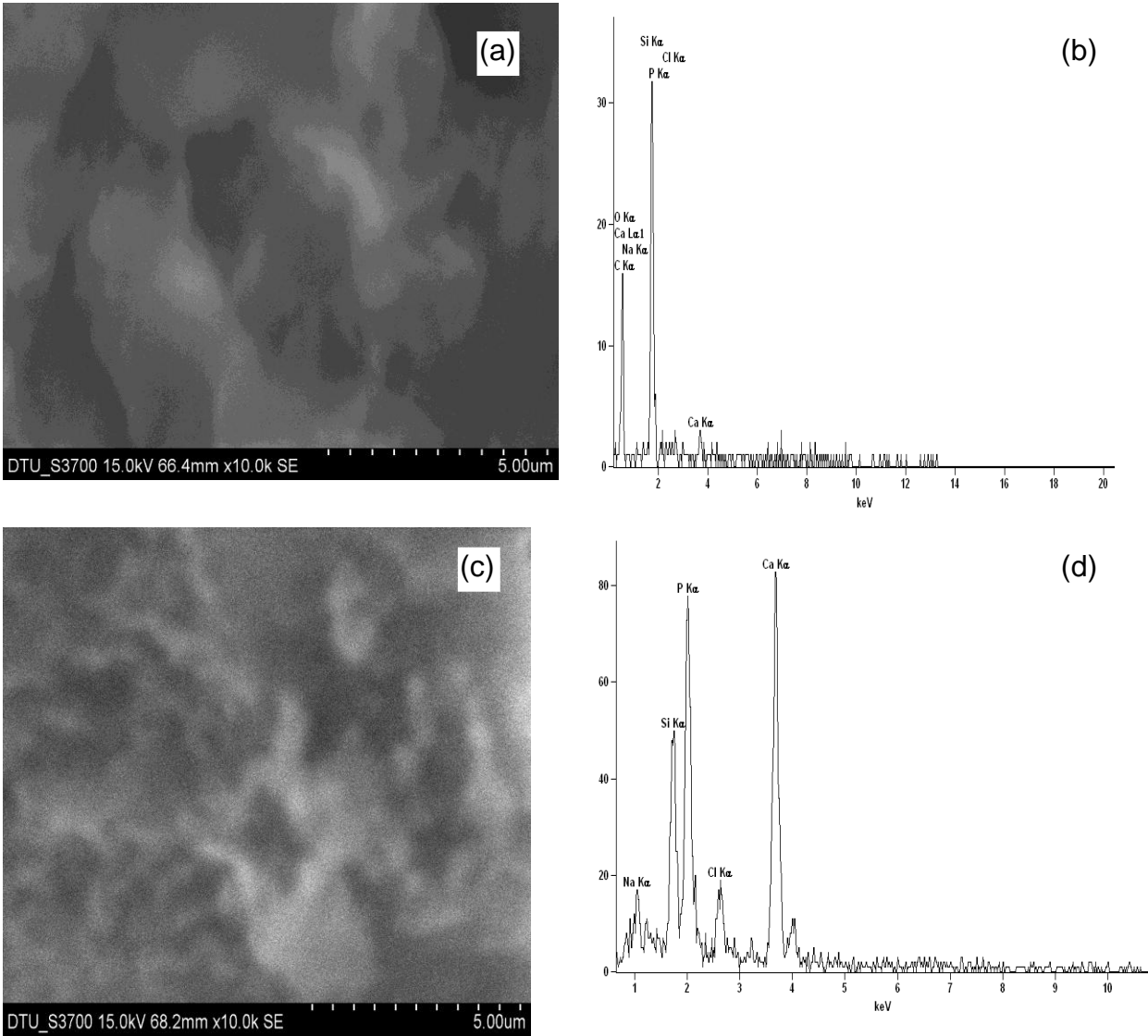
Fig. 4.22. SEM (HITACHI S-3700N) micrographs (a) and (c) as well as EDS spectra (Thermo scientific NORAN) ((b) and (d)) showing surface morphological analysis of bioglass BIG-BG-G after (a,b) 0 day (d,e) 30 days. interaction with SBF

Figure 4.23 (a) shows SEM (HITACHI S-3700N) micrographs of bioglass (SG-BG-G) surface morphology before interaction with SBF, the surface looks clear from precipitate and is explained in detail already (Figure 4.9 (a)). On the other hand, the corresponding sample morphology after 30 days interaction with SBF (Figure 4.23 (c)) shows a white precipitate on the surface, Which is further confirmed by EDS spectrum (Figure 4.23 (d)) showing Ca and P Peaks indicating the precipitation of hydroxy apatite after interaction with SBF.
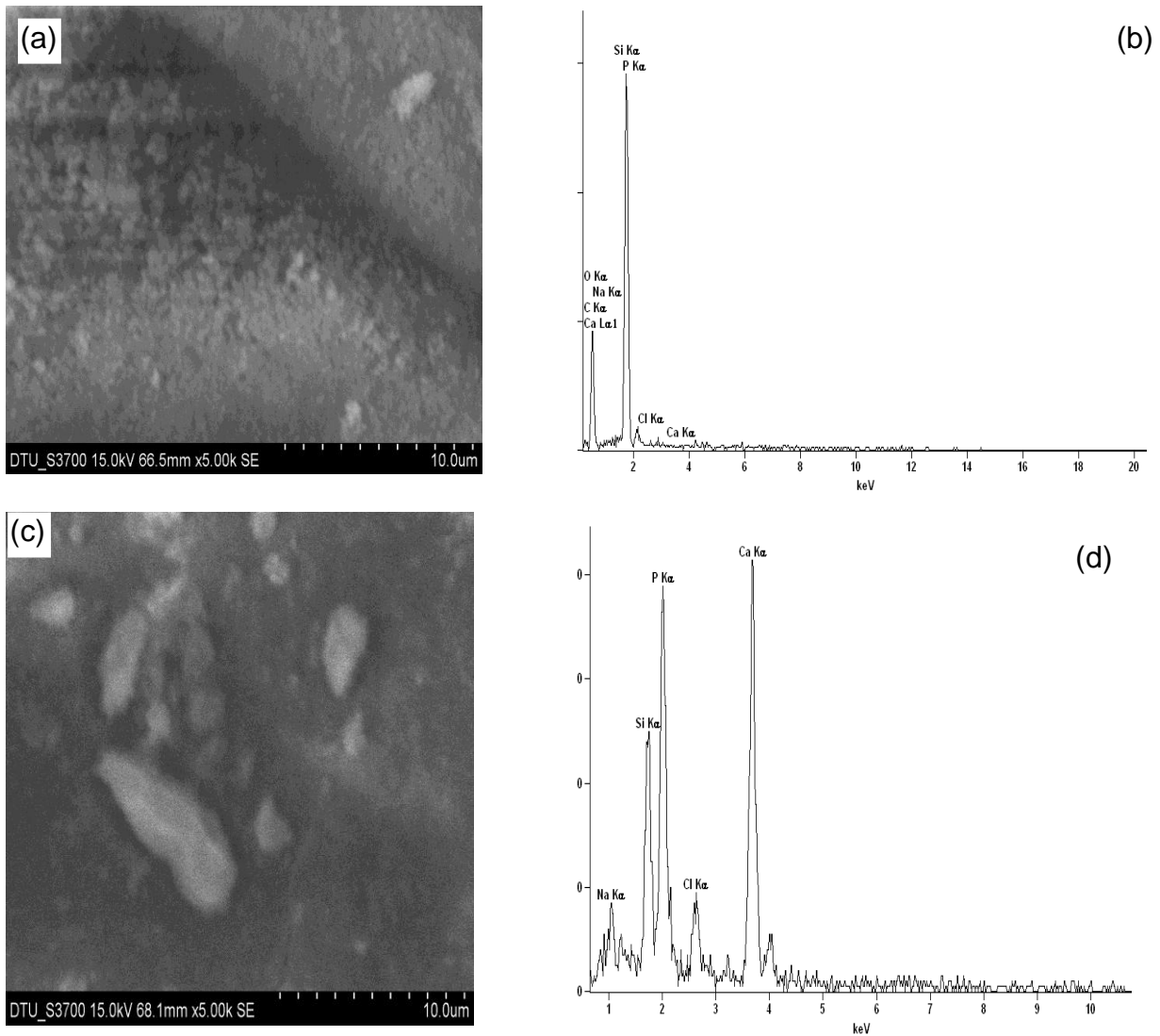
Fig.4.23. SG-BG-G SEM (HITACHI S-3700N) micrographs (a) and (c) as well as EDS spectra (Thermo scientific NORAN) ((b) and (d)) showing surface morphological analysis of bioglass SG-BG-G after (a,b) 0 day (d,e) 30 days interaction with SBF.

Figure 4.24 shows concentration of Ca and P released from the bio glass BIS-BG-D before and after interaction with SBF and corresponding pH values. Interestingly pH of SBF solution increase from 7 to 8.3 after 7 days and remain at that value more or less constant till 30 days indicating release of calcium and phosphorous ions from the bioglass sample. It is pertinent to mention that release of Ca and P ions from the bioglass sample also show similar trend to the observed pH changes in SBF during

interaction with the bioglass and results are in good agreement with earlier findings [84]. The observed increase in pH and release of ion further confirm the precipitation of hydroxyl carbonated apatite (HCA) on surface of the biomaterial.
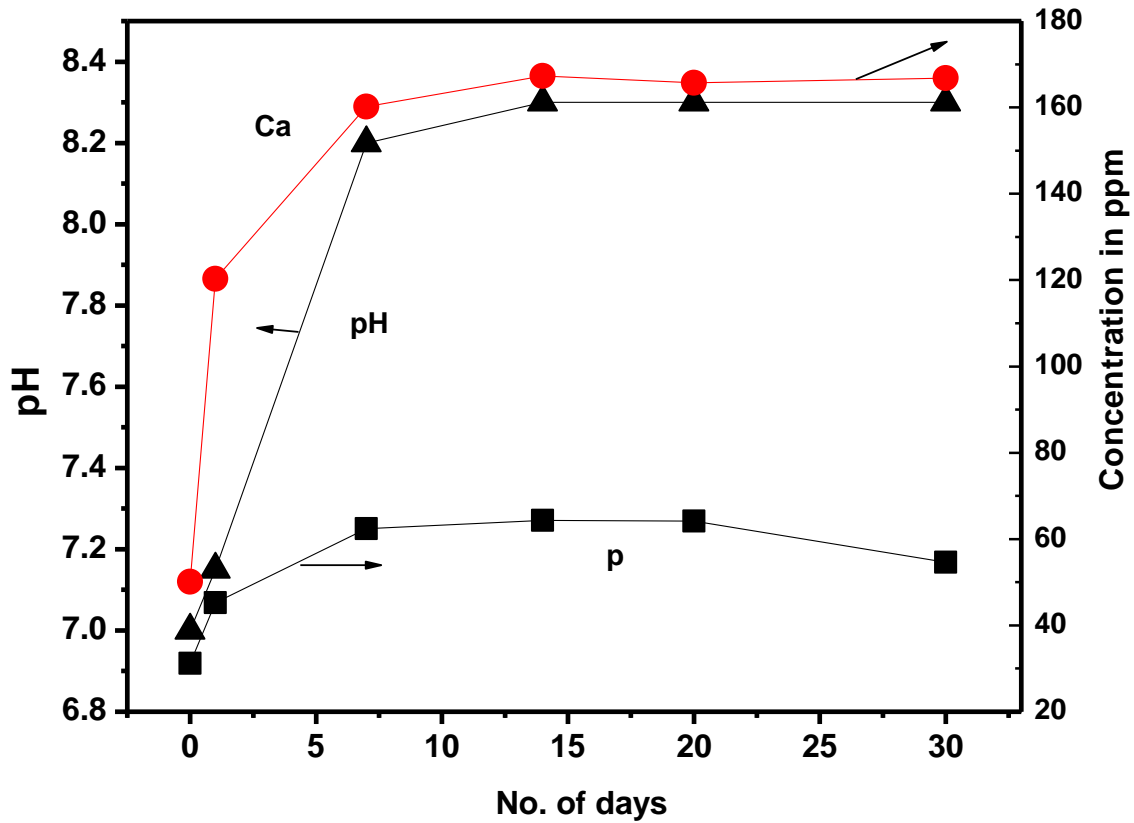
Fig.4.24. Analysis of Ca and P in ppm before and after interaction of BIS-BG-D with SBF

The cell cytotoxicity was carried out by MTT assay and the results are displayed in Figure 4.25. In these experiments, a human osteoblast-like osteosarcoma cells grown in DMEM medium is considered as a positive control and the medium in the absence of cell is taken as negative control. In the presence of the extract of BIS-BG-D nearly about 90% cells are alive after incubation with the extract. Hardy about 8% difference between the cell growth in absence and in the presence of cell is expected and in good

agreement with the other researchers [85, 111-113]. The optical micrograph of the osteosarcoma cells before and after contact with the bioglass show almost similar morphology, further supports for the good cytocompatibility of the BIS-BG-D bioglass.
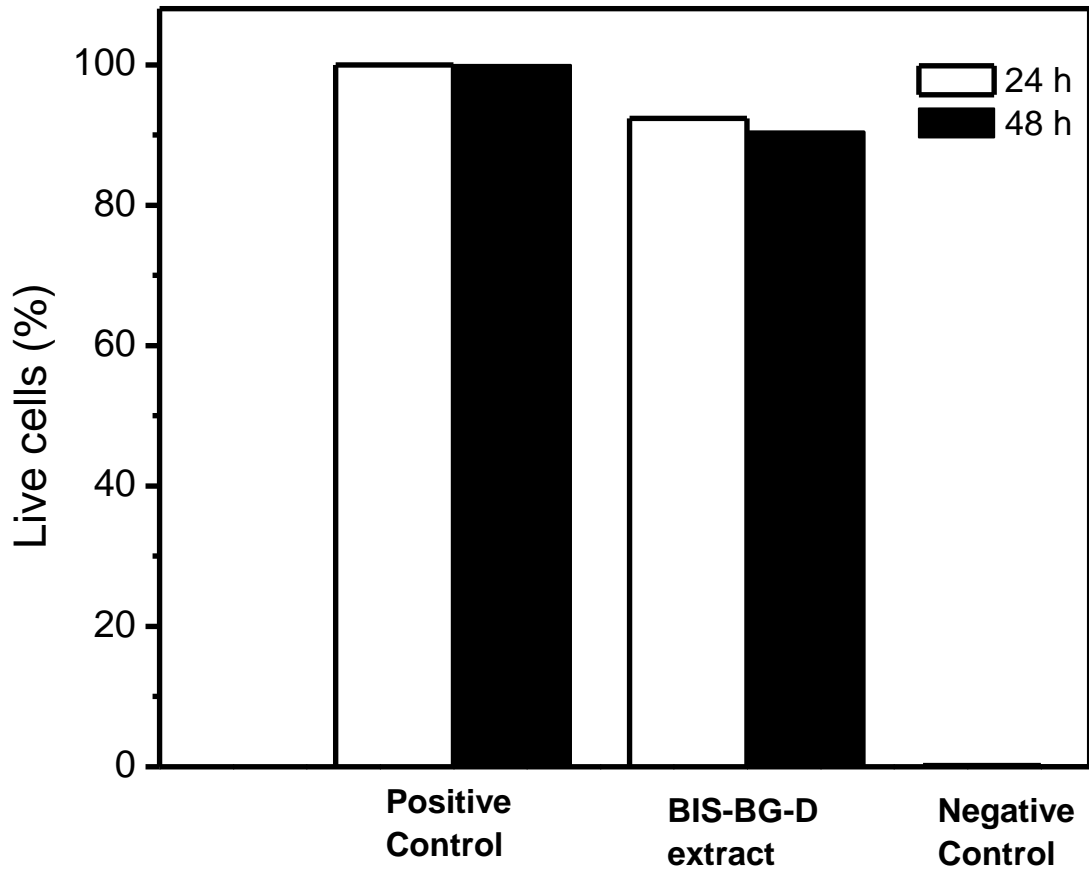
Fig.4.25. MTT assay showing biocompatibility of BIS-BG-D
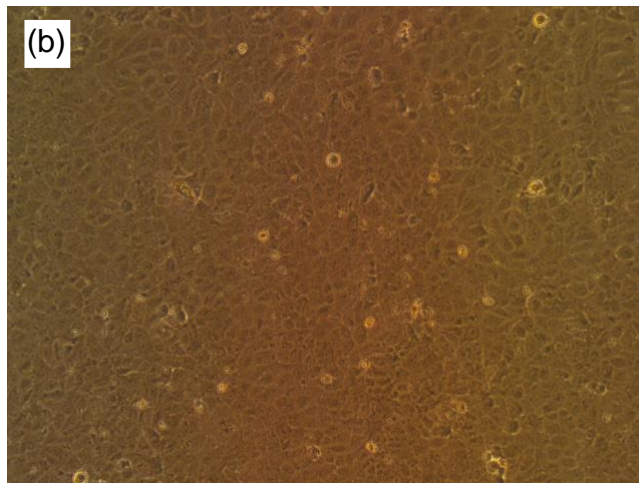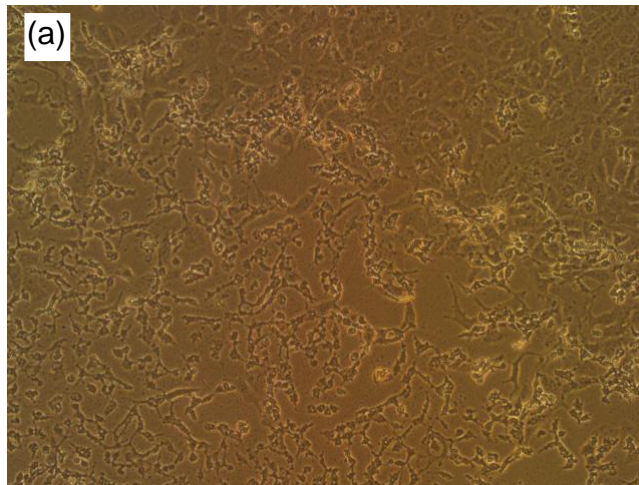
Fig.4.26. Morphology of the cells (a) not in contact and (b) in direct contact with BIS-BG-D

5.Conclusions

Bioactive glass (BIS-BG-D and BIS-BG-G) are prepared more economically and eco-friendly way by bioinspired method using CT-DNA/glelatin as template. Additionally a bioglass named SG-BG-G is also prepared by traditional sol-gel rout using gelatin. All these three samples are characterized by FTIR, XRD and SEM. XRD analysis reveals that glasses prepared by bioinspired method are found to be partially crystalline in nature compared to the glass sample SG-BG-D, which is amorphous. Interestingly, SEM results show that the bioglass BIS-BG-D is mesophorous in nature, which is expected due to the existence of coiled conformation of CT-DNA in the presence of positively charged ions in the medium, compared to the biomaterials BIS-BG-G and SG-BG-G. Other tests, such as density measurements showed bioglass prepared by sol-gel rout is of highest density due to the calcination of the sample, in vitro degradation as well as swelling studies indicate that the glasses prepared by bioinspired rout are found to degrade as well as swell easily compared to the glass obtained by sol-gel method in which calcination of the sample carried out. The higher degradation and swelling of the bioactive glasses prepared by bioinspired rout indicate favorable atmosphere for the growth of bone cells. More interestingly, the growth of hydroxyl carbonated apatite (HCA) deposition is observed in in vitro bioactivity test on the surface of all bioglass samples by immersing them in SBF. It is pertinent to mention that, the bioactive glass sample BIG-BG-D is found to show higher in vitro bioactivity compared to other samples due to its mesoporous microstructure. Importantly, the cell cytotoxicity tests carried out using osteosarcoma cells on BIS-BG-D extract as well as on the pellet indicate that the bioglass prepared by bioinspired method indicate the biocompatibility of the glass sample. Additionally, the cell morphology is observed to be retained before and after interaction with the bioglass. These observations provide information that bioinspired rout is a promising, ecofriendly and cheaper method to synthesis third generation biomaterials, which serve as in vitro tissue engineering scaffold to repair bone tissues.

6. Future Scope

(1) Using bioinspired rout bioactive glass samples of various composition as well as textures of interest required for in-vitro tissue engineering scaffolds (such as Fibers, films etc.) are possible to synthesis.

(2) In-vitro tissue engineering test on the biomaterials can be carried out and the corresponding genotoxicity can also be tested for the same.

REFRENCES

(1)	Williams, D.F. Ed. (1987), Definitions in Biomaterials. In progress in biomedical engineering, 4, 67. Edited by D.F. Williams, Elsevier, Amsterdam.

(2)	Biomaterials, S.V. Bhat, second edition, Narosa publishing house 2005.

(3)	L.L. Hench The story of bioglass. J. Mater Sci: Mater Med (2006) 17: 967-978

(4)	Kokubo T. Recent progress in glass-based materials for biomedical applications. J. Ceram. Soc. Jpn (Seramikkusu Ronbunshi) 1991; 99: 965-73

(5)	L.L. Hench, R.J. Splinter, W.C. Allen and T.K. Greenlee J. Biomed. Mater.Res. 1971, 5, 117

(6)	P. N. De Aza, A.H. De Aza, P. Pena and S. De Aza, Bioactive glasses and glass-ceramics, Bol. Soc. Esp. Ceram. V., 46 (2) (2007).

(7)	O.P. Filho, G.P. La Torre and L. L. Hench, "Effect of crystallization on apatite layer formation and bioactive glass 45S5",J. Biomed. Mater. Res., 30, 509-514 (1996)

(8)	P. Saravanapavan and L.L. Hench J. Non-Cryst Solids, 2003, 318, 1.

(9)	P. Saravanapavan and L.L. Hench J. Non-Cryst Solids, 2003, 318, 14.

(10)	Jones JR. New trends in bioactive scaffolds: the importance of nanostructure. J. Eur Ceram Soc 2009; 29:1275

(11)	Li R, Clark AE Hench LL., An investigation of bioactive glass powders by sol-gel processing J. Appl Biomater 1991; 2(4) 231-9.

(12)	Dillow, A. K. and Lowman, A.M. (2002), Biomimetics Materials and Design. Marcel Dekker, New York..

(13)	Dujardin, E.; Mann, S. Adv. Matter, 2002, 14(11), 775-778

(14)	Mann S. Nature, 1993, 365, 499.

(15)	Lu, X. Y.; Lim S. W. J. Am. Chem. Soc., 2003, 125, 888

(16)	Hench L L Sol-gel material for bioceramic applications, Curr Opin Solid State Mater Sci 1997 2 604.

(17)	L.L. Hench, Paschall H.A. (1973) J. Biomed Mater Res 7: 25-42.

(18)	T. Kokubo, H. –M. Kim and M. Kawashita, Biomaterials, 2003, 24, 2161.

(19) Best SM, Porter AE, Thain ES, Huang J. Bioceramics; Past, Present and for the future, J. Eur Ceram Soc 2008: 28; 1319.

(20) Aldo R. Boccaccini, Melek Erol, Wendelin J. Stark, Dirk Mohn, Zhongkui Hong, Joao F. Mano, Polymer/bioactive glass nanocomposites for biomedical applications: A review. Composites Science and Technology 70 (2010) 1764-1776.

(21) Segtnan, V.H.; Isaksson, T. Food hydrocolloids 2004, 18, 1-11

(22) Petia Atanasova et al., DNA-templated synthesis of ZnO thin layers and nanowires Nanotechnology 20 (2009) 365302 (7pp)

(23) Introduction to biomedical engineering, John Enderle, Susan Blanchard, Joseph Bronzino (Eds.), Academic Press, California 2005.

(24) Integrated Biomaterials Science, (Ed) Rolando Barbucci, Plenum Publishers, New York 2002

(25) Hench L.L. and Wilson, J. (1993) An introduction to bioceramics. (Advanced series in bioceramics Vol. 1.) World scientific, River Edge, New Jersey.

(26) Park, J.B. and Bronzino, J.D. (2003) Biomaterials Principles and Applications. CRC, Boca Raton, Florida.

(27) Ratner, B.D., Hoffman, A.S., Schoen, F.J. and Lemons, J.E. (2004) Biomaterial Science: An iintroduction to Materials in Medicine. 2nd edition, Academic Press. San Diego, California.

(28) Mann S. (1996) Biomimetic Materials Chemistry, VCH Pulishers, New York

(29) Rho,J-Y., Kuhn-Spearing, L. and Zioupos, P. (1998) Mechanical properties and the hierarchical structure of bone. Med. Engineering and phys 20, 92-102

(30) Katja Hoehn, Marieb, Elaine Nicpon (2007) Human Anatomy and Physiology (7th edition) San Francisco: Benjamin Cummings.

(31) Bryan H, Derrickson, Tortora, Gerard J. (2005) Principles of anatomy and physiology New York, Willy.

(32) Bhasker S.N. Cutright D.E. Knapp M.J. Beasley J.D. Perez B. and Driskel T.D. (1971) Tissue reaction to intra bony ceramic implants, Oral surg. Oral Med. Oral Pathol, 31, 382.

(33) Black J. (1980) Biological performance of Materials, Dekkar, New York.

(34) Aragona, J. Parson, J.R., Alexander, H., Weiss, A.B., Clin.Orthop.1981, 160, 268.

(35) Temenoff J.S. Lu L., Mikos A.G. Bone tissue engineering using synthetic biodegradable polymer scaffolds In: Davies J.E. editor. Bone engineering Toronto: EM squared; 2000, p.455-62.

(36) Bruder S.P. Caplan A.I. Bone regeneration through cellular engineering In: Lanza R.P. Langer R, Vacanti J, editors. Principles of tissue engineering 2nd ed. California: Academic Press, 2000, p. 683-96.

(37) L.L. Hench. 'Bioactive ceramics'. In Bioceramics Materials characteristics versus In vivo Behaviour, Eds. P. Ducheyne and J.E. lemons, Annals of New York Academy of science, New York, Vol 523, 54, (1988).

(38) Freyman TM, Yannas IV, Gibson LJ. Cellular materials as porous scaffolds for tissue engineering. Prog Mater Sci 2001; 46: 272-82.

(39) H.-M. Kim Ceramic bioactivity and related biomimetic strategy. Current opinion in solid state Materials science 7 (2003) 289-299.

(40) Kokubo T, Miyaji F, Kim H.M. Nakamura T. Spontaneous formation of bonelike apatite layer on chemically treated titanium metals. J. Am. Ceram soc. 1996, 79:1127-9.

(41) L. L. Hench, J. Wilson and D. C. Greenspan J. Aust. Ceram. Soc., 40(1) (2004) 1.

(42) P. N. De Aza, A.H. De Aza, P. Pena and S. De Aza, Bioactive glasses and glass-ceramics, Bol. Soc. Esp. Ceram. V., 46 (2) 45-55 (2007).

(43) L.L. Hench Bioceramic From Concept to Clinic, J. Am. Ceram. Soc., 74[7] 1487-1570 (1991).

(44) M.M. Walter, An investigations in to the bonding mechanism of bioglass, Master thesis, University of Florida, Gainsville (1977)

(45) Ogino M, Hench L. L. (1980) J. Non-cryst Solids. 38-39 Part 2: 673-678.

(46) J. Wilson, A. Yli-Urpo and R. P. Happonen, in An introduction to bioceramics ed. L. L. Hench and J. Wilson, world Scientific, Singapore, 1993, pp. 63-73.

(47) I. Kinnunen, K. Aitasalo, M. Pollonen and M. Varpula, Journal of Cranio Maxillofacial surgery, 2000, 28, 229.

(48) Hench L. L. (1998) J. Am. Ceram Soc. 81:1705-1728.

(49) M. J. Peltola, J. Suonpaa, K. M. J. Aitasalo, M. Verpula, A. Yi-Urpo and R. P. Happonen, Head Neck, 1998, 20, 315

(50) M.J. Peltola, K.M.J. Aitasalo, A.J.Aho, T. Tirri and J.T.K. Suonpaa J. Oral Maxillofacial Surg., 2008, 66, 1699.

(51) Q.Z. Chen, I.D. Thompson and A. R. Boccaccini, Biomaterials, 2006, 27, 2414.

(52) L.G. Griffith and G. Naughton,, Science, 2002, 295, 1009.

(53) V.A. DUbok Bioceramics-yesterday, Today, Tomorrow, Powder Metallurgy and Metal Ceramics, Vol. 39, Nos 7-8, 2000.

(54) Sepulveda P, Jones JR, Hench LL Characterization of melt derived 45S5 and sol-gel-derived 58S Bioactive glasses. J. Biomed Mater Res 2001: 58(6) 734-40.

(55) Saravanapavan P. Jones J R, Pryce RS, Hench L. L. J. Biomed Mater Res A 2003:66A(1) 110-9.

(56) W. Xia, J. Chang Mater. Lett. 61 (2007) 3251-3253

(57) Petil O., LaTorre GP, Hench LL, J. Biomed Mater Res 1996 30 509

(58) Petil O., Zanotto ED Hench LL J. Non-cryst solids 2001:292 115

(59) Clupper DC Mecholsky JJ, LaTorre GP., Greenspan DC J. Biomed Mater Res 2001 57 532.

(60) Clupper DC Mecholsky JJ, LaTorre GP., Greenspan DC Biomaterials 2002 23 2599.

(61) Carta D.,Pickup DM, Knowles JC, Smith ME J. Mater Chem. 2005 15-2134

(62) Chen QZ, Rezwan K ,Francon V, Armitage D,Nazhat SN, Jones FH,et al.Surface function of bioglass((R))-Derived porous scaffolds. Acta Biomater 2007;3:551.

(63) Lefebvre L., Gremillard L., Chevalier J. Bernache-Assolant D. (2008) Sintering behavior of 45S5 Bioglass (R), Bioceramics Vol 20, Pts 1 and Pts 2, pp 265-268.

(64) Lefebvre L Chevalier J. Gremilland L., Zenati R., Tholler G., Bernache-Assolant D. Govin A (2007) Acta mater 55: 3305-3313.

(65) Nychka J A, Mazur S, Kashyap S, Li D, Yang FQ (2009) JOM-US. 61: 45-51.

(66) Jones JR, Sepulveda P. Hench L. L. (2001) J Biomed Mater Res 58(6) 720-726.

(67) Yan XX, Yu CZ, Zhou XF, Tang JW, Zhao DY. Angew Chem Int Ed 2004;43:5980–4.

(68) Shi QH, Wang JF, Zhang JP, Fan J, Stucky GD. Adv Mater 2006;18:1038–42

(69) Hongsu Wang , Xiaohan Gao , Yanan Wang , Jinglong Tang , Cancan Sun , Xuliang Deng , Xiaodi Niu , Materials Letters 76 (2012) 237–239

(70) X.X. Yan, C.Z. Yu, X.F. Zhou, J.W. Tang, D.Y. Zhao, Angew. Chem., Int. Ed. 43 (2004) 5980.

(71) Q.H. Shi, J.F. Wang, J.P. Zhang, J. Fan, G.D. Stucky, Adv. Mater.18 (2006) 1038.

(72) A. Lopez-Noriega, D. Arcos, I. Izquierdo-Barba, Y. Sakamoto, O.Terasaki, M. Vallet-Regi, Chem. Mater. 18 (2006) 3137.

(73) M. Hartmann, Chem. Mater. 17 (2005) 4577.

(74) M. Vallet-Regı´, Chem.dEur. J. 12 (2006) 5934.

(75) Yufang Zhu , Chengtie Wu, Yogambha Ramaswamy , Emanuel Kockrick ,Paul Simon , Stefan Kaskel , Hala Zreiqat, Microporous and Mesoporous Materials 112 (2008) 494–503

(76) X. Yan, C. Yu, X. Zhou, J. Tang, D. Zhao, Angew. Chem., Int. Ed. 43 (2004) 5980.

(77) X.X. Yan, H.X. Deng, X.H. Huang, G.Q. Lu, S.Z. Quio, D.Y. Zhao,C.Z. Yu, J. Non-Cryst. Solids 351 (2005) 3209.

(78) X. Yan, X. Huang, C. Yu, H. Deng, Y. Wang, Z. Zhang, S. Qiao, G. Lu, D. Zhao, Biomaterials (2006) 3396.

(79) W. Xia, J. Chang, J. Controlled Release 110 (2006) 522.

(80) Q. Shi, J. Wang, J. Zhang, J. Fan, G. Stucky, Adv. Mater. 18 (2006) 1038.

(81) T.A. Ostomel, Q. Shi, C.K. Tsung, H. Liang, G.D. Stucky, Small 2 (2006) 1261.

(82) Q Z Chen, Guo C Zaho N.,Appl. Sur. Sci. 2008, 255, 456-8

(83) Saravanapavan P, Hench L L Key Eng Mat 2003 240-242, 213.

(84) Chen QZ, Ahmed I., Knowles JC, Nazhat SN, Boccaccini AR Rezwan K. J. Biomed Mater Res Part A 2008, 86A, 987.

(85) Chen QZ, Li Y, Jin LY, Quinn MW, Komesaroff PA, Acta Biomaterialia 6 (2010) 4143-4153.

(86) Kokubo T and Takadama H Biomaterials 27 (2006) 2907-2915

(87) Xynos ID, Edgar AJ, Buttery LDK, Hench LL and Polak J.M. J. Biomed Mater Res. 2001 55, 151.

(88) O. Tsigkau, Jones J. R., Polak JM and Sievens M. M. Biomaterials 2009, 30, 3542.

(89) El-Ghannam A. Ducheyne P., Shapiro IM (1997) Biomaterials 18(4) 295-303.

(90) Kaufmann EA, Ducheyne P, Radin S. Bonnell DA Composto R (2000) J. Biomed Mater Res 52 825-830

(91) Buchanan LA, El-Ghannam A. (2010) J. Biomed Mater Res Part A 93(2) 537-546

(92)   Bahniuk MS, Pirayesh H, Singh HD, Nychka JA, Unsworth LD Biointerphases (2012) 7 41.

(93)   Chitra Vaid, Sevi Murugavel, Raman Kashayap, Ram Pal Tandon, Synthesis and in vitro bioactivity of surfactant template mesoporus sodium silicate glases, Microporous and Mesoporous Materials 159 (2012) 17–23

(94)   Hench L. L. Theory of bioactivity: the potential for skeletal regeneration. Anales de Quim 1997; 93, 544

(95)   Hench L.L. Wilson J. Surface active biomaterials, Science 1984: 226, 630

(96)   Kokubo T., Hata k., Nakamura T., Yamamura T. Apatite formation on ceramics, metals and polymers induced by a CaO-SiO2- based glass in simulated body fluid In: Bonfield W. Hastings CW, Tanner KE, editors. Bioceramics. Vol 4. London: Butterworth-Heinemann; 1991, p. 113.

(97)   M. Peter, N.S. Binulal, S.V. Nair, N. Selvamurugan H. Tamura and R. Jayakumar, Chemical Engineering Journal 158 (2010) 353-361.

(98)   H.Aguiar, J. Serra, P. Gonzalez, B. Leon, J. Am. Ceram. Soc. 93(2010)2286-2291.

(99)   M.Prassas, J. Phalippou, L.L. Hench, J. Zarzycki, J. Non-Cryst. Solids 48 (1982) 79-95.

(100)   H.Aguiar, J.Serra, P. Gonzalez, B. Leon, J. Non-Cryst. Solids 355(2009)475-480.

(101)   Socrates, G., Infrared Characteristic Group Frequencies Willey-Interscience, New York, 1980

(102)   Ferraro, J.R., and Basi Le, Infrared Spectroscopy, Academic Press, New York, 1978.

(103)   Herman, A.S., Infrared Hand Book, Plenum, New York, 1963.

(104)   Bauermann LP, Bill J and Aldinger F, Bio-friendly synthesis of ZnO nanoparticles in aqueous solution at near-neutral pH and low temperature, J. Phys.Chem. B 2006, 110, 5182-5185.

(105)   Bauermann LP, del Campo A, Bill J and Aldinger F, Heterogeneous Nucleation of ZnO using gelatin as the organic matrix, Chem. Mater. 2006, 18, 2016-2020.

(106)   Gerstel P, Hoffmann RC, Lipowsky P, Jeurgens LPH, Bill J and Aldinger F, Mineralisation from aqueous solutions of zinc salts directed by amino acids and peptides, Chem. Mater. 2006, 18, 179-186.

(107) Gerstel P, Lipowsky P, Durupthy O, Hoffmann RC, Bellina P, Bill J and Aldinger F, Deposition of zinc oxide and layered basic salts from aqueous solutions containing aminoacids and dipeptides, Journal of the ceramic society of Japan 2006, 114(11) 911-917.

(108) D. Santhiya, Z. Burghard, L.P.H. Jeurgens, J. Bill and F. Aldinger Deposition of TiO_2 thin films on hydrophobin and its nanomechanical properties, Langmuir 26, 6494-6502 (2010).

(109) Kokubo T. Bioactive glass ceramics properties and applications. Biomaterials 1991; 12: 155-63.

(110) C. Vaid and S. Murugavel, In vitro bioacvtivity of sol-gel prepared silicate glasses, J. Mater. Sci. and Engg. (submitted)

(111) Saravanapavan P, Selvakumaran J, Hench L.L. Bioceramics 16, 2004, 254-2 785

(112) Saravanapan P, Jones JR, Verrier S., Beilby J.J. Shirtiff VJ Hench LL et al., Bio Med mater Eng 2004 14 467.

(113) Stanley HR, Hall MB, Clark AE, King CJ, Hench LL Berte JJ Int J Oral Maxillofacial implants 1997: 12 95.